universität wien

MASTERARBEIT / MASTER'S THESIS

Titel der Masterarbeit / Title of the Master's Thesis

„How is cohesin regulated by post-translational modifications during mammalian meiosis?"

verfasst von / submitted by

Andrea Hirsch BSc.

angestrebter akademischer Grad / in partial fulfilment of the requirements for the degree of

Master of Science (MSc)

Wien, 2016 / Vienna 2016

Studienkennzahl lt. Studienblatt / degree programme code as it appears on the student record sheet:	A 066 877
Studienrichtung lt. Studienblatt / degree programme as it appears on the student record sheet:	Masterstrudium Genetik und Entwicklunsbiologie / Master's degree programme Genetics and Developmental Biology
Betreut von / Supervisor:	Dr. Kikue Tachibana-Konwalski
Mitbetreut von / Co-Supervisor:	/

Acknowledgments

I would like to take this opportunity to express my sincerest gratitude to Dr. Kikue Tachibana-Konwalski, who gave me the chance to gather new experiences in an exciting field of research.
I am thankful for her guidance and the many inspiring and enlightening discussions we had throughout the process.
Further I would like to thank my colleagues for their support during my many hours in the lab, with special thanks to Anna Szydlowska-Bylicka.

I owe my deepest gratitude to my parents, my sister and my beloved partner who supported me in every possible way and made my studies even possible.

Zusammenfassung

Um eine korrekte Chromosomenverteilung während Mitose und Meiose zu ermöglichen, müssen neu replizierte Schwesterchromatiden eng zusammengehalten werden. Dieser Zusammenhalt, genannt Kohäsion, wird gewährleistet durch das binden von Multiprotein Cohesin Komplexen an doppelsträngige DNA, um sie so ringförmig zu umschließen und zu verknüpfen. Aufgrund des verzögerten meiotischen Zellzyklus in weiblichen Organismen, muss die Schwesterchromatidenkohäsion in Mäusen für Wochen oder Monate und im Menschen sogar über Jahre oder Jahrzehnte sichergestellt werden. Um die Integrität einer gesunden Eizelle zu schützen, müssen Cohesin Komplexe so lange gebunden bleiben, bis der meiotische Zellzyklus fortsetzt wird, was wiederum eine strenge Regulation von Cohesin vorraussetzt. Ein essentielles Protein, genannt Smc1β, wurde als Bestandteil von Cohesin in Mäusen identifiziert. Aufgrund bisheriger Studien wird vermutet, dass Smc1β eine Funktion während der meiotischen Rekombination erfüllt und für den Erhalt der Kohäsion der Schwesterchromatiden erforderlich ist. Wie der meiotische Cohesin Komplex in Säugetieren durch post-translationale Proteinmodifikationen reguliert wird, ist nicht bekannt. Wir zeigen, dass bestimmte post-translational modifizierte Aminosäuren in Smc1β notwendig sind, um seine Funktion während der meiotischen Rekombination zu erfüllen und Schwestercentromere zusammenzuhalten. Wir beobachten eine Rolle von Smc1β während der Verteilung und effizienten Reifung von Cross-overs in fötalen Eizellen. Smc1b ist notwendig für die korrekte Assoziation von Schwesterkinetochoren von Chromosomen während der Diakinese. Dies lässt auf eine Rolle von Smc1b in centromerer Kohäsion schließen. Unsere Studie gewährt Einblicke in die Regulierung von Cohesin Komplexen, welche Smc1β enthalten. Wir schlussfolgern, dass post-translationale Modifikationen die Funktion der meiotischen Cohesin Komplexe während meiotischer Rekombination und Schwesterchromatidenkohäsion regulieren.

Abstract

Holding together replicated sister chromatids is an essential requirement for proper chromosome segregation during mitosis and meiosis. This so-called sister chromatid cohesion is established through cohesin, a ring-like multiprotein complex that embraces double-stranded DNA. Due to the prolonged meiotic cell cycle of mammalian females, sister chromatid cohesion needs to be maintained for weeks or months in mice or in humans for years or decades. This presupposes a tight regulation of factors responsible for chromatid cohesion in order to preserve the genomic integrity of a healthy oocyte. One essential component of the mice meiotic cohesin complex is Smc1β. Smc1β is thought to be involved in meiotic recombination and required for maintenance of sister chromatid cohesion. How meiotic cohesin is regulated by post-translational modifications in mammalian meiosis is not known. Using mouse genetics, we show that specific residues that are post-translationally modified are necessary for Smc1β's function in meiotic recombination and centromeric cohesion. We find that Smc1β affects cross-over distribution and efficiency of cross-over maturation in fetal oocytes. Smc1β is required for close association of sister-kinetochores in meiosis I diakinesis oocytes, suggesting that it is involved in centromeric cohesion. Thus, our study provides insights into the regulation of Smc1β-containing cohesin complex. We propose that post-translational modifications regulate the function of the meiotic cohesin complex during meiotic recombination and sister chromatid cohesion.

Table of Contents

The generation of a haploid reproductive cell

The formation of a mature and healthy oocyte represents the basic foundation for the generation of new life. Haploid reproductive cells are formed in a specialized cell cycle named meiosis (Alberts et al. 2005). In mammals, of sexually reproducing species fusion of sperm and egg gives rise to a diploid organism (reviewed by Longo F.J. 1973). The way of an immature primary oocyte to a fertilizable egg is highly regulated to ensure proper development of the embryo.

Mammalian meiosis and gametogenesis

Meiosis is a specialized cell cycle that is characterized by a single genome replication followed by two cell divisions. It is required to generate cells with a haploid genome that can fuse during sexual reproduction in order to form a diploid cell and thereby ensures chromosomal integrity of a diploid embryo (Sun and Cohen 2013; Alberts et al. 2005). The meiotic cell cycle is conserved in every eukaryotic organism and can be found in both female and male mammals whereas the timing of particular events is variable during their distinctive gametogenesis (Alberts et al. 2005).

In male testis, meiosis is continuously initiated by spermatogonial stem cells (SSC), which self-renew or enter meiosis to form an immature spermatid followed by spermatogenesis (Handel et al. 2010; Bohacek et al. 2015). In contrast, female meiosis is initiated only once in a finite amount of oogonial cells during embryonal development and arrests during prophase I until it is reactivated after entering puberty at the day of ovulation (reviewed by Von Stetina and Orr-Weaver 2011).

For both females and males, the generation of a haploid cell starts with a pre-meiotic S-phase where the DNA of a diploid parental cell is replicated in order to result in a cell with a 4C DNA content, 2 chromatids per chromosome (Fig. 1) (Handel et al. 2010). This is followed by prophase I, which can be further divided into specific events based on the alignment of homologous chromosomes by a unique proteinaceous scaffold structure, the synaptonemal complex (SC) and the formation of cross-over (CO) between homologous chromosomes

(Smith et al. 2001; reviewed by Marston and Amon 2004; Sun and Cohen 2013). During the first phase of meiotic prophase I, the leptonema, chromosomes begin to condense and chromosomes start searching for their homologs. Subsequently the assembly of the first proteinaceous filament of the SC between the chromosome pairs is initiated (Bisig et al. 2012; reviewed by Baudat et al. 2013; Sun and Cohen 2013). Stepwise the formation of the SC continuous during zygonema and pachynema, the second and third phase of prophase I. By the end of the pachytene event homologous chromosomes are completely aligned by the synaptonemal complex and cross–over designated sites are determined (Fig.1) (reviewed by Handel et al. 2010). During the next phase, the diplonema, the components of the SC start to be removed again between the homologous chromosomes (Bisig et al. 2012) to ensure that by the stage of diakinesis chromosome pairs are only connected through their chiasmata and the centromere (reviewed by Marston and Amon 2004).

During female development, oocytes enter prophase I before birth and after entering diplotene, cells arrest at the dictyotene stage until puberty (Gilbert SF. 2000). Five days after birth the whole pool of oocytes have entered the dictyate phase. During this time oocytes remain in a quiescent-like stage and the primordial follicle is formed (reviewed by McLaughlin and McIver 2009; Sun and Cohen 2013). From the beginning of this stage oocytes are surrounded by a single layer of epithelial granulosa cells and mesenchymal-like cells forming the primordial follicle. These cell layers start to grow periodically and also the dormant oocytes increase in size, resulting in a fully grown multilayer follicle of granulosa cells with an embedded 500-fold bigger oocyte (Gilbert SF. 2000). Entering the reproductive life initiates the exit of selected oocytes of the dictyate phase and resuming meiosis at each estrous cycle. Within a mouse lifetime only a few oocytes release their dormant state during estrous initiation which implies that a pool of oocytes remain in the quiescent stage for weeks or months (Sun and Cohen 2013). Looking particularly at the human cycle, which can be described with similar course of events, cells need to be arrested for years or decades (reviewed by Handel and Schimenti 2010; Von Stetina and Orr-Weaver 2011; Toth and Jessberger 2016).

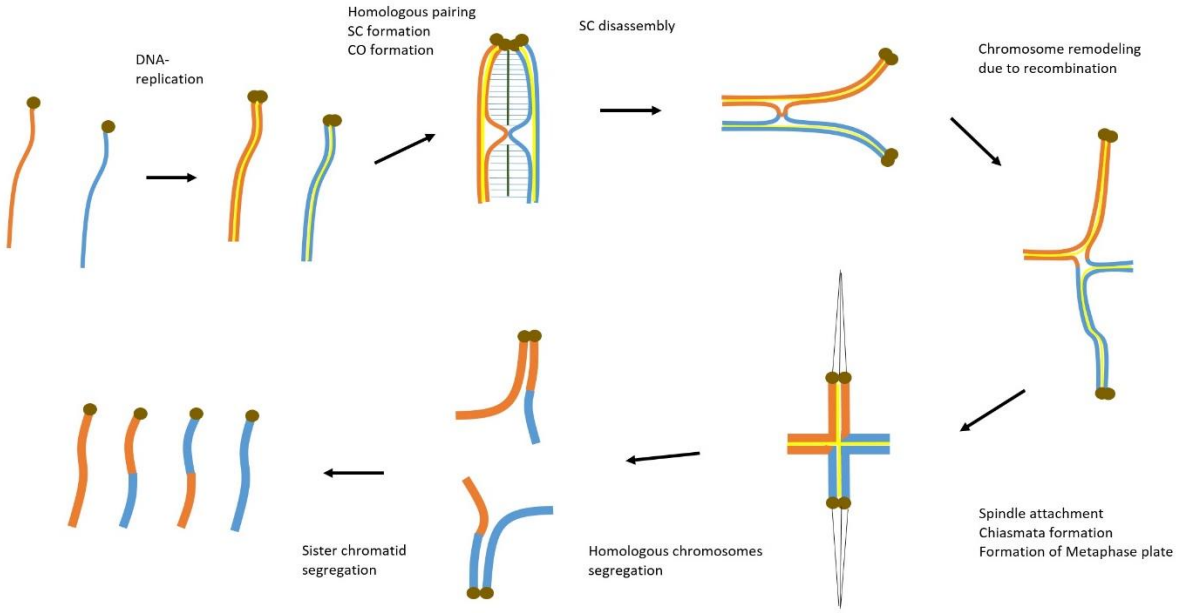

Figure 1. Model of chromosome organization during mammalian meiosis. For simplicity chromosome organization during meiosis is shown for one pair of homologous chromatids, a maternal (orange) and paternal (blue) chromatid. DNA replication initiates the establishment of sister chromatid cohesion (yellow) and with the onset of meiotic prophase I the SC components start to assemble and form synapsis between homologs. After CO formation the SC components disassemble to enable chromosome remodeling to facilitate recombination. In metaphase I the meiotic spindle attaches (black) and chiasmata become visible. After assembly at the metaphase plate homologous chromosomes segregate. The second meiotic division proceeds without previous replication, resulting in 4 haploid meiocytes. (Model adapted from Martinez-Perez et al. 2009)

After re-entering the meiotic cell cycle, oocytes undergo the first meiotic division which results in the formation of a haploid cell and the first polar body, both containing one set of chromosomes (2C DNA content). The second meiotic division is initiated at fertilization of the haploid egg without DNA replication. Sister chromatids segregate in anaphase II (Fig. 1). The second polar body is formed and the fertilized oocyte remains with a haploid set of maternal and paternal chromatids (reviewed by Handel and Schimenti 2010).

The synaptonemal complex – an unique meiotic proteinaceous scaffold

During mammalian meiosis homologous chromosomes pair and recombination between a maternal and paternal homolog occur to ensures chromosome segregation and genetic diversity in the newly formed cell. To facilitate a stable pairing of homologous chromosomes during Prophase I the synaptonemal complex (SC) is formed between their two axes (Smith et al. 2001; reviewed by Handel and Schimenti 2010). It is a proteinaceous tripartite structure that links the two homologs together and enables a controlled cross-over formation between them (Kouznetsova et al. 2011; Syrjänen et al. 2014; Yang et al. 2009; Smith et al. 2001). A failure of SC formation can have several tremendous consequences for the meiotic progression of a germ cell resulting in infertility of the organism or aneuploidy in the haploid cell (Yuan et al. 2002).

The formation of the SC starts during the first Prophase I sub-stage, the Leptonema, with the assembly of a lateral element (LE) along the chromosome axes, also called axial element (AE). The two lateral axes of a homologous pair are then 'zipped' together through the alignment of transverse filaments (TF) and central element (CE) components, building the central regions (CR) in Zygonema (reviewed by Fraune et al. 2012). Together the lateral element and the central region represent the synaptonemal complex and with entering the pachytene event, homologous chromosomes are completely aligned by the SC (Fig. 2) (Bisig et al. 2012).

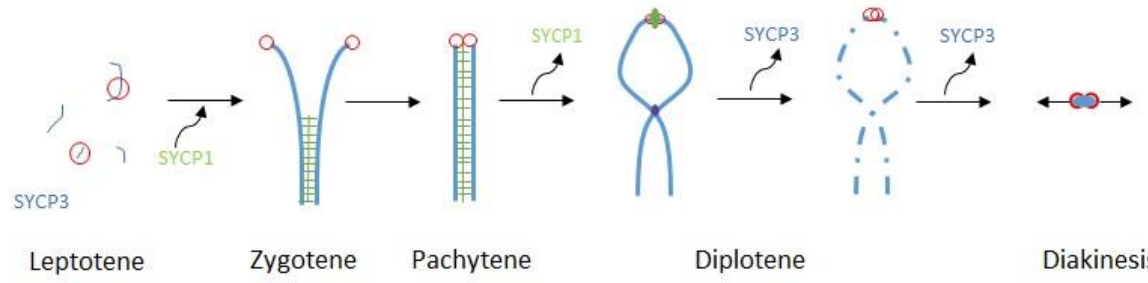

Figure 2. Model of synaptonemal complex formation during meiotic prophase I. In leptotene components of the SC start to assemble along chromosome axis and by SYCP1 the axial elements get zipped together to form complete synapsis between homologs in pachytene stage. After CO formation SYCP1 and SYCP3 disassemble from chromosome axis and only SYCP3 remains at the centromere until chromosomes bi-orient and segregate in diakinesis. (Model adapted from Bisig et al. 2012)

After a programmed DNA double strand break (DSB), catalyzed by a conserved Topo-VI-like tetrameric enzyme (Spo-11) (reviewed by Robert et al. 2016), the loading of two recombinases (RAD51 and DMC1) initiates the searching for the homologous sequence (reviewed by Baudat et al. 2013). After assembly of meiosis-specific cohesin core components along two neighbouring homologous chromosome axes the LE is formed between them by two components, SC protein 2 (SYCP2) and SYCP3 that can interact with each other by forming heterodimers (Garcia-Cruz et al. 2010; Schalk et al. 1998; Yang et al. 2006). The 'zipping' of the two AE is achieved through the binding of the TF-specific protein, SC protein 1 (SYCP1) (Fig. 2). Two SYCP1 molecules start to interact with each other via N-terminal head to head junctions and the binding of CE-specific proteins (SYCE1, SYCE2, SYCE3 and TEX12) complete the formation of synapsis (reviewed by Fraune et al. 2012; Hernández-Hernández et al. 2016). Independent of the axial components assembly, the HORMA domain-containing protein HORMAD1 binds to the unsynapsed homologous chromosome axes at the site of DSB initiation (Fukuda et al. 2010). After strand invasion, catalyzed by RAD51 and DMC1, several single-strand DNA binding proteins bind and SC formation begins (reviewed by Baudat et al. 2013). HORMAD1 stays until TF components start to assemble (Fukuda et al. 2010) while recombination intermediates start to get processed, entering either the cross-over pathway via a double Holiday junction formation or the non-cross-over pathway via single-end strand invasion. The first pathway needs to be resolved in the next step by the assembly of specific proteins, the MutL protein homolog 1 (MLH1), MLH3 and the exonuclease 1 (EXO1) during pachynema (reviewed by Baudat et al. 2013). Entering diplonema leads to the degradation of SC components, starting with the reduction of SYCP1 along the arms in early diplonema but maintaining at the centromere until entering late-diplonema. The same is true for SYCP3, starting degradation in late-diplonema along chromosome arms but persisting at the centromere until Anaphase I (Bisig et al. 2012).

The formation of the axial element is furthermore provided by the assembly of the meiotic cohesin complex.

Cohesin – the ring that mediates sister chromatid cohesion

During meiotic progression sister chromatids stay associated until they segregate in anaphase II (Martinez-Perez et al. 2009). To ensure correct distribution of genomic DNA within the newly formed daughter cell, sister chromatid cohesion must be maintained until onset of anaphase II. As mentioned previously female oocytes stay in an arrested stage until they re-enter meiotic progression (Sun and Cohen 2013), while sister chromatid cohesion needs to be maintained for weeks or months in mice or in humans for years or decades (Tachibana-Konwalski et al. 2010; Burkhardt et al. 2016). During DNA replication cohesin complexes embrace sister chromatids leading to a close association. Sister chromatid cohesion (SCC) persists until the homologous chromosomes separate in anaphase I, starting with the removal of cohesin complexes along the chromosome arms whereas sister centromeres stay associated. Sister kinetochores are mono-oriented ensuring that the kinetochores are captured by microtubules emanating from the same spindle pole (reviewed by Nasmyth and Haering 2009).

The core cohesin complex is composed of two SMC (structural maintenance of chromosome) proteins, SMC1 and SMC3, each forming an intermolecular antiparallel α-helical coiled-coil structure. Both SMC proteins contain a 'hinge' domain, located in the middle of their protein structure followed by the back-fold intertwined structure and their collateral N- and C-terminal domains (reviewed by Jessberger 2002). For both SMC isoforms the N-terminus interacts with the C-terminus forming a nucleotide-binding domain (NBD). These rod-like structures, SMC1 and SMC3, can interact with each other via their hinge domain forming a V-shape complex ending with the two associated NBD in order to form an ABC transporter-like adenosine triphosphatase (ATPase)-head domain. This ATPase-head domain offers binding sites for two ATP molecules, to further catalyze their hydrolysis (reviewed by Strunnikov and Jessberger 1999; reviewed by Nasmyth and Haering 2009; latest described by Ladurner et al. 2014 for mammals).

To establish cohesion of two sister chromatids, cohesin complexes are loaded onto DNA through the interaction with several proteins. The binding of the third cohesin component an α-kleisin protein, called RAD21/SCC1 in mammals, to both ends of the Smc proteins leads to

the formation of a ring like structure. Furthermore the binding of the last core component, SA (stromal antigen) protein, completes the core cohesin complex (Losada et al. 2000; reviewed by Nasmyth and Haering 2009).

In order to guarantee a dynamic but stable sister chromatid cohesion at the same time, the loading, the maintenance and release of cohesin complexes need to be highly regulated. This regulation is facilitated through the binding of specific regulator proteins. The mammalian proteins PDS5A and PDS5B represent two isoforms of the PDS5 protein that contain tandem sequence repeats (HEAT-repeats) (reviewed by Nasmyth and Haering 2009). These HEAT motifs can be found in various chromosome-associated proteins and in particular they were also found in the yeast cohesin loader SCC2 and in non-SMC proteins functioning as an important interface for protein interactions (Ono et al. 2003). In different organisms, Pds5 and its isoforms were identified as a cohesin interacting partner which thereby regulate the cohesin complex in different ways (Neuwald et al. 2000). Whereas in yeast, *Drosophila* and *C.elegans* the orthologues protein of Pds5 plays a major role for the maintenance of sister chromatid cohesion (Hartman et al. 2000; Dorsett et al. 2005; Wang et al. 2003), it seems that Pds5 has a dual function in vertebrate cells acting as a stabilizer or as a destabilizer of cohesin complexes (Losada et al. 2005).

The second cohesin interacting partner was first described in *Drosophila* as a regulator of heterochromatin organization and of sister chromatid cohesion, named WAPL (wings-apart like) (Vernì et al. 2000). Six years later an ortholog of the *Drosophila* WAPL protein was identified in vertebrates, functioning as a regulator of SCC (Kueng et al. 2006; Gandhi et al 2006). WAPL can interact with the cohesin core complex through the binding to the α-kleisin subunit and the SA protein.

Sororin represents another cohesin interactor that was so far only described in vertebrates (Rankin et al. 2005). It functions through the interaction with WAPL in order to inhibit the releasing activity of it and thereby stabilizes cohesin on the chromatin (Ladurner et al. 2016).

The meiotic cohesin complex

During the first stages of meiosis the newly synthesized sister chromatids synapse with their homolog. The alignment of chromatids and formation of inter-sister cohesion is provided through the recruitment and assembly of specific meiotic cohesin components.

Different isoforms of the cohesin core components were identified to be responsible for the establishment of SCC during Meiosis and Mitosis. In *S.pombe* the entering into meiosis initiates a replacement of the mitotic cohesin complex by meiosis specific components (Ding et al. 2016). Also in meiotic mammalian cells, specific paralogs of the mitotic cohesin components SMC1α, RAD21 and STAG1-2, were found. SMC1β represents the meiotic SMC1 which distinguishes from SMC1α through a basic C-terminal domain (Revenkova et al. 2001). Recent studies suggest that SMC1β could be also expressed in somatic tissue (Mannini et al 2015). Like SMC1α it interacts together with SMC3 and both cohesin complexes, the mitotic and meiotic one, could be immunoprecipitated from meiotic mammalian cells (Revenkova et al. 2001).

First described in yeast is an alternative α-kleisin subunit, called REC8. Like the mitotic ortholog, REC8 is important to prevent SCC during meiotic progression. REC8 can either form a complex with SMC3/SMC1β or SMC3/SMC1α (Eijpe et al. 2003). REC8 containing cohesin complexes starts to establish sister chromatid cohesion during DNA replication (Lee et al. 2003; Burkhardt et al. 2016). REC8 persists on the chromatin axis until the onset of anaphase I. Concurrently, when the chromosomes start to separate, REC8 is removed from the chromosome arms but remains within the centromeric regions until metaphase II (Lee et al. 2003). Depletion of Rec8 provoke various meiotic dysfunctions, including defective chromosome segregation, a reduction in sister chromatid cohesion and an aberrant recombination frequency (Klein et al. 1999; Molnar et al.1995; Watanabe and Nurse 1999). Subsequently, an orthologue of the yeast Rec8 was identified in mammals and *C.elegans* to be important for SC formation and SCC (Parisi et al. 1999; Pasierbek et al. 2001).

A third alternative kleisin subunit was identified in mammalian meiocytes, sharing homologous structures with the two α-kleisin subunits RAD21 and REC8, named Rad21-like protein (RAD21L). A scenario was reported illustrating an exchange of cohesin complexes

containing RAD21 with complexes that can either contain RAD21L or REC8 starting during premeiotic S-phase. RAD21L can further form a cohesin ring with both SMC1 subunits, SMC1α and SMC1β (Gutiérrez-Caballero et al. 2011). Following meiotic progression and looking at prophase I, a co-localization of RAD21L can be observed with the AE and LE until mid pachytene. Given the observations, that RAD21L remains on the SC until mid pachytene and is then again replaced, indicates a role of RAD21L during initiation of synapsis and recombination (Lee et al. 2011). Besides the association of RAD21L with the SMC1 paralogs this kleisin subunit can also interact with SMC3 and the meiosis-specific stromalin protein STAG3 (Gutiérrez-Caballero et al. 2011). Described for human and mice, STAG3 represents a meiotic version of the mammalian mitotic stromalin proteins. It contains the characteristic stromalin conservative domain (SCD), which can be found in every member of the stromalin protein family (Pezzi et al. 2000). During male meiosis STAG3 can be observed for the first time in late stages of leptotene and persists at the chromatin axis until anaphase I. When homologous chromosomes need to get separated in anaphase I cohesin complexes including STAG3 is removed from the chromosome arms but persist at the sister centromere region. With the onset of metaphase II STAG3 is completely removed and not detectable anymore (Prieto et al. 2001).

When both meiotic kleisin subunits (REC8 and RAD21L) are defective, no STAG3 or SMC1β assembly is detectable in leptotene, whereas the cohesin component SMC3 and the mitotic kleisin RAD21 can be observed. This indicates a REC8/RAD21L dependent cohesin ring complexation with SMC1β and STAG3 (Llano et al. 2012). The fact that the mitotic kleisin subunit RAD21 is also detectable prior to the pachytene stage represents contradictory results to the postulated model of a RAD21 exchange with RAD21L during premeiotic S-phase until early leptotene (Parra et al. 2004; Ishiguro et al. 2011; Herrán et al. 2011). The fact that during leptotene in Rec8 KO spermatocytes the SCC formation is impaired, but restored during meiotic progression (thought by RAD21L), indicates an important role of REC8 establishing canonical SCC whereas RAD21L has its major role in synapsis of the homologs (Ishiguro et al. 2014).

How is cohesin regulated during mitosis and meiosis?

Proper chromosome segregation during the mitotic and meiotic division is essential to preserve the chromosomal integrity of the newly formed daughter cell. The loading of different composed cohesin complexes on the chromatin, happening during different cell cycle stages, and their maintenance provides a stable association of homologous chromosomes until they separate in anaphase. To prevent premature separation of homologous chromosomes and to ensure a correct sister chromatid cohesion the loading and the removal of cohesin complexes is under close surveillance by various protein complexes. The regulation of cohesin by these proteins either function through protein-protein interactions or posttranslational modifications of cohesin components.

Smc3 acetylation by Eco1 is essential for establishing sister chromatid cohesion

SMC3 is loaded onto DNA during premeiotic S-phase, forming a functional cohesin complex together with SMC1α and REC8 (Eijpe et al. 2000) or with SMC1β in order to facilitate chromatid cohesion. The importance of Eco1 (**E**stablishment of **Co**hesion) for chromatid cohesion was already reported for yeast (Tóth et al. 1999), where it was described as a protein that contains a zinc-finger domain and regulates the establishment of cohesion by its acetyltransferase activity (Ivanov et al. 2002; Unal et al. 2008). Further studies resolved that Eco1 is not needed to load cohesin complexes onto chromatin but via catalyzing the acetylation of the two Smc3 lysine residues, K112 and K113, a close association of the cohesin complex with the DNA gets initiated. Synchronously with the DNA replication, acetylation of those specific lysine residues by Eco1 can be observed in order to stabilize cohesin complexes along the sister chromatids (Tóth et al. 1999; Ben-shahar et al. 2008). The human orthologue ESCO1 and a second acetyltransferase, ESCO2, were identified displaying similar function in mammalian cells by catalyzing two lysine residues, K105 and 106, of SMC3 (Zhang et al. 2008). It was reported that in mammalian cells cohesin complexes get stabilized along the DNA through an interaction of cohesin and the cohesin interactor protein sororin after SMC3 acetylation (Ladurner et al. 2016).

Stable binding of the cohesin complex by the interacting protein named sororin

Sororin, named initially p35, was first identified as a regulator of sister chromatid cohesion working during the mitotic cell cycle (Rankin et al. 2005). This cohesin interacting partner is so far only described for vertebrates in order to stabilize cohesin complexes on chromatin (Schmitz et al. 2007; Kim et al. 2013). The different sororin orthologs do not display high sequence similarities suggesting not an essential role of sororin for sister chromatid cohesion (Nishiyama et al. 2010). Partially that was the case, since it was shown that cohesin can be loaded independently of sororin onto DNA (Nishiyama et al. 2010) but its maintenance requires the interaction with sororin (Ladurner et al. 2016). Recently the work of Ladurner et al uncovered the function of sororin, getting recruited by acetylated SMC3 solely onto DNA after replication. Through a phenylalanine-glycine-phenylalanine (FGF)-motive within a conserved region of sororin, it binds to PDS5 in order to prevent the premature release of cohesin by WAPL (Ladurner et al. 2016; Nishiyama et al. 2010). The association of sororin with Pds5 and Wapl leads to a restructuring of Pds5-Wapl heterodimer to allow a stable cohesin binding along the DNA (Nishiyama et al. 2010). With the onset of metaphase cohesin is released from the chromatin to allow chromosome segregation. Therefore, sororin is inactivated which is facilitated through a posttranslational modification. Phosphorylation of sororin due to mitotic entry abolishes the inhibition of Wapl in order to initiate cohesin removal from chromosomes (Nishiyama et al. 2010).

Pds5 a cohesin interacting partner conserved from yeast to human

Two Pds5 like proteins were identified, named PDS5A and PDS5B, in vertebrates displaying properties similar to those of Pds5 in yeast and fungi (Losada et al. 2005; Hartman et al 2000). Human PDS5A and B show sequence similarities within their N-terminal region, both containing HEAT-repeats, followed by a conserved region and a divergent C-terminus (Losada et al. 2005). In *Xenopus* egg extract the C-terminal region of Pds5B contains target sites for Cdk phosphorylation, which differentiates it from Pds5A and thereby regulates the binding of cohesin complexes. For both Pds5 isoforms a high binding affinity with the cohesin complex was identified (Losada et al. 2005). Depletion of either Pds5A or B

displayed conflicting phenotypes relative to Pds5A and B double knock-out (Zhang et al. 2007). It seems that Pds5 can either function on the cohesin complex in a positive or negative way, which suggests a complex function of Pds5 in regulation of chromatid cohesion (Losada et al. 2005).

WAPL – the opposing factor in order to release cohesin

The human protein, named WAPL, is an ortholog of the Drosophila wings-apart like protein (Wapl) (Kueng et al. 2006). In Drosophila, WAPL was identified to play a role during heterochromatin formation (Vernì et al. 2000; Oikawa et al. 2004). The structure of WAPL orthologs is conserved within vertebrates displaying an N-terminal region with a FGF-motive and an α-helical C-terminus. It was assumed that this particular N-terminus takes over a regulatory function (Shintomi and Hirano 2009). Similar motives were already described for other proteins were it was shown that through these motives proteins can bind to HEAT-motives (Bayliss et al. 2000). The fact that Wapl and sororin display both FGF-motives and Pds5 contains HEAT-domains already indicates that these have protein binding partners (Shintomi et al. 2009; Nishiyama et al. 2010; Losada et al. 2005).

WAPL is a direct interacting partner of PDS5A, forming a heterodimer that interacts with cohesin through the binding to the kleisin subunit (Kueng et al. 2006). Despite the association of sororin, WAPL remains bound to PDS5A, however a structural conformation change of the heterodimer is induced (Nishiyama et al. 2010). Thereby the function of WAPL is repressed from telophase until prophase. With the onset of Metaphase, sororin gets posttranslational modified which leads to an abolishment of WAPL inhibition and a cohesin removal by WAPL (Nishiyama et al. 2010; Kim et al. 2013).

During the mitotic cell cycle cohesin is removed in two stages. First cohesin is released on chromosome arms mediated by a so called ‘Prophase-Pathway’. This pathway includes the phosphorylation of sororin by Cdk1 and Wapl activation (Kitajima et al. 2006; Nishiyama et al. 2013). The posttranslational modified sororin is removed from cohesin facilitated by Aurora B and thereby the conformation of the heterodimer Wapl-Pds5 is changed in a way that cohesin gets removed by Wapl (Nishiyama et al. 2010). Simultaneously centromeric

cohesin complexes need to be stabilized in order to prevent precocious chromosome separation. Phosphorylation of sororin, located at the centromeric region, is protected by the shugoshin- phosphatase 2A protein complex (Sgo1-PP2A) (Nishiyama et al. 2013). Secondly, with the onset of Metaphase Sgo1-PP2A disappear from the centromeric region and at the metaphase to anaphase transition the anaphase-promoting complex/cyclosome (APC/C) is activated. APC/C is an E3 ubiquitin ligase which can mark diverse proteins for degradation via ubiquitination. One of its target protein is the separase inhibitor securin, that gets ubiquitinated in order to release separase. Activated separase cleaves the remaining cohesin complexes at the centromere in order to allow chromosome segregation (Manchado et al. 2010; reviewed by Ishiguro and Watanabe 2007).

During the first meiotic division homologous chromosomes separate but sister chromatid cohesion persists until Anaphase II. One mechanism explaining how this is regulated was described for fission yeast. The meiosis specific kleisin subunit Rec8 is posttranslational modified by the kinase CK1 and Cdc7 along the chromosome arm. This phosphorylation mark is required for the followed cohesin cleavage at the chromosome arm whereas centromeric cohesion is not changed. At the centromere Rec8 is protected against phosphorylation due to Sgo1-PP2A association (Riedel et al. 2006). In Anaphase II this protection is abolished and Rec8 can be cleaved by separase (Brar et al. 2006; reviewed by Watanabe 2012; Ishiguro and Watanabe 2007).

The cohesin subunit Smc1β

When the Smc1 subunit, SMC1β, was first identified in 2001 by Revenkova et al. this protein was defined as a novel meiosis-specific isoform of Smc1 that represents high homology with Smc1α and contains a characteristic basic C-terminal domain (Revenkova et al. 2001). Within the following years function, interaction with different binding associates were identified and its role during meiosis was determined.

SMC1β was isolated from mouse testis as a 150-kDa interacting partner protein of SMC3. A C-terminal domain flanks one side of a coil-coiled structure containing 28aa with specific

basic amino-residues. The rest of the protein structure is comparable with Smc1α, containing an N-terminal domain representing together with the C-terminal domain an ATPase head. In the middle of the protein a domain functions as a flexible hinge in order to facilitate a folding back of the coil-coiled structure in an interwined parallel manner (Revenkova et al. 2001). While Smc1β shares common characteristics with Smc1α, it displays a unique pattern during meiosis indicating an individual role of SMC1β in meiocytes (Revenkova et al. 2001; Eijpe et al. 2003; Revenkova et al 2004). A scenario were cohesin is loaded onto chromatin before meiotic S-phase, related to the model of cohesin loading at premitotic S-phase and establishment of cohesion during S-phase in mitotic yeast (Uhlmann and Nasmyth 1998) is provided by the diffuse pattern of the cohesin complex Smc1-Smc3-Rec8 (Eijpe et al. 2000). The distribution of cohesin complexes, containing SMC1α, in pre-meiotic S-phase and the following dot-like assembly along AE indicates an important function of SMC1α cohesin complexes in cohesion establishment (Eijpe et al. 2003). The cohesin complex containing SMC1β represents a quite different localization during meiosis. Initially SMC1β starts to assemble after pre-meiotic S-phase along the AE. Concurrently with SMC3, SYCP3 and SYCP2, SMC1β can be observed for the first time in leptotene (Eijpe et al. 2003) and persists along the chromatin axis until diplotene. With the onset of metaphase I SMC1β is removed from chromosome arms but remains together with SMC3 at the centromere until anaphase II (Revenkova et al. 2001). This specific localization was described in spermatocytes, whereas in metaphase I oocytes SMC1β is detectable along the chromosome axis with a higher incidence at the centromeric region (Kouznetsova et al. 2005). While SMC1α can never be detected at the centromere during meiosis, the unique pattern of SMC1β indicates an important function for maintenance of cohesin and centromeric cohesion (Revenkova et al 2001; Biswas et al. 2013).

The distinctive pattern of SMC1β indicates a specific role of it during meiosis, individually for male and females. The generation of genetic knockouts revealed SMC1β's function. Genetic knockout of SMC1β results in a healthy but sterile organism despite a normal mating behavior. In male mice this is due to the lack of spermatids. Looking closer at the development of spermatocytes reveals an arrest of their maturation during mid-pachytene with a synaptonemal complex half its size of a wild-type (WT) meiocyte. The fact that the short

AE are flanked by a telomere structure and a centromere structure indicates a different general chromatin organization during SC formation within this mutant and not a fragmentation of the SC. This is also provided by the increased extensions of chromatin loops along the SC (Revenkova et al. 2004). Looking at female meiosis within a SMC1β deficient mice, 'mature' oocytes can be found with increased aneuploidy, resulting in sterility of the female. Female meiosis is not arrested during a specific meiotic stage, as described for the male meiosis, and oocytes reach the dictyate stage in the end. Similar to the male phenotype, the SC is remarkably reduced and due to the premature loss of cohesion chromosomes have problems to segregate properly (Revenkova et al 2004; Hodges et al. 2005).

Smc1β knockout mice display a second phenotype affecting meiotic recombination. Meiotic recombination starts with a programmed double-strand break during leptotene, get then processed through the binding of specific recombination intermediate proteins and in the end resolved through the interaction of MLH1, MLH3 and EXO1 (reviewed by Baudat et al. 2013). In order to study and observe recombination defects in mutant mice these binding proteins can be used to detect crossover formation. To analyze recombination defects in SMC1β deficient mice the MutL protein MLH1 was used to localize recombination sites (Revenkova et al. 2004), which appear under normal conditions from early- to mid-pachytene (reviewed by Baudat et al. 2013). In the *Smc1β* $^{-/-}$ spermatocytes no MLH1 foci were detectable, which could be due to the premature arrest in a pachytene-like stage (Revenkova et al. 2004). In male meiosis detectable MLH1 foci have only a short time frame, appearing strictly during mid-pachytene (De La Fuente et al. 2012). Since factors responsible for recombination initiation appear normally within the mutant, the absence of MLH1 foci could be due to an arrest (Revenkova et al. 2004).

In *Smc1β* $^{-/-}$ oocytes the progression through meiosis I enables the observation of cross-over-designated sites through immunolabeling of pachytene cells for MLH1. In SMC1β depleted oocytes a reduced number of MLH1 foci can be observed, suggesting a reduction of cross-over events due to the loss of one cohesin complex component (Revenkova et al. 2004; Hodges et al. 2005). The decrease of MLH1 foci in female oocytes and an overall absence of it in spermatocytes indicates a role of SMC1β during recombination individually for males and females.

To explain the discrepancy between SMC1β depleted male and female meiocytes one might need to take in account the overall more stringent regulation of male meiosis than female meiosis (reviewed by Hassold and Hunt 2001). The fact that depletion of SMC1β leads to a meiotic arrest of male meiosis whereas female oocyte progress through the first meiotic events indicates a much more stringent surveillance of the male meiotic cell cycle (Revenkova et al. 2004). This observation is further provided by the existence of a pachytene checkpoint, that gets activated if meiotic recombination is initiated but not completed, resulting in meiotic arrest followed by apoptosis (Roeder et al. 2000). Why SMC1β depleted oocytes continue to progress through meiosis is not clear so far, therefore one can only speculate whether a specific checkpoint is not triggered efficiently.

To study further the function of SMC1β during meiotic recombination, the localization of MLH1 foci in pachytene oocytes was determined and compared to the sites of chiasmata in diakinesis oocytes. A shift was observed within *Smc1β* $^{-/-}$ oocyte from normal distributed MLH1 signals, which were comparable to the WT, to much more distally located chiasmata in the diakinesis oocytes (Hodges et al. 2005). The fact that in *Smc1β* $^{-/-}$ oocytes MLH1 foci can be observed and in further stages chiasmata are present indicates not an essential role of SMC1β for CO formation during female meiosis (Revenkova et al. 2004; Hodges et al. 2005). However the results postulated by Hodges and his colleagues suggests a function of SMC1β in maintaining CO events throughout the meiotic progression (Hodges et al. 2005).

Furthermore, a correlation of SC length and reduced number of MLH1 foci was reported. Similar to the male phenotype, the axis length of the SC was visibly reduced in *Smc1β* $^{-/-}$ oocytes. The depletion of SMC1β resulted in a 30% shorter SC in the mutant oocytes relative to the WT, which is less short than for the *Smc1β* $^{-/-}$ spermatocytes (50%). The fact that in the mutant oocytes recombination is reduced by nearly the same extend (25%) this might be the result of a direct relationship between recombination and length of the SC (Hodges et al. 2005).

The third phenotype described by Hodges et al. was based on their observation of univalents in oocytes of a one-month old mutant. When they examined oocytes from *Smc1β* $^{-/-}$ mice of different ages, they were able to observe an age-related increase of univalents and single

chromatids. This represents the evidence that SMC1β is required for maintenance of sister chromatid cohesion in an age-dependent manner (Hodges et al. 2005).

The fact that the phenotype generated by SMC1β depletion cannot be compensated by SMC1α cohesin complexes suggests an important role of SMC1β for SCC maintenance and meiotic progression.

Although in SMC1β depleted meiocytes the telomere structure can be detected on both sides of the synaptonemal complex, despite its altered length, those cells reveal several telomeric defects (Adelfalk et al. 2009). During the meiotic cell cycle telomeres usually stay attached to the inner nuclear membrane. With the onset of leptotene the telomeres get linked to the nuclear envelope through the interaction with specific cytoskeletal and motor proteins (Chikashige et al. 2007; Schmitt et al. 2007). Via these motor proteins the telomeres can move along the nuclear periphery in order to bring them together clustering in a bouquet-configuration. With the entrance into zygotene telomeres are again disseminated over the nuclear periphery indicating a role of this pattern during homologous chromosome pairing and meiotic recombination (Scherthan et al. 2007). Through the bouquet formation homologous chromosomes are brought in close proximity to each other, facilitating an efficient alignment of the homologs (Harper et al. 2004).

Depletion of Smc1β leads to defective telomere attachment to the nuclear envelope which can be seen as an increase of telomere ends located to the inner mass of the cell (Hodges et al. 2005). In total ~17% of the telomere ends had problems to attach to the nuclear periphery. Furthermore, the overall structure of the telomere was impaired resulting in ends of SC filaments that completely lack specific telomere proteins. Additionally, in almost every mutant cell, during zygotene to pachytene transition, telomeres can be found with a stretched pattern. Those stretched structures were also observed to occur between two telomere ends representing a bridge-like configuration. All these telomere aberrations are not a result of a decline of interaction between nuclear membrane proteins and the SC or the altered axis length. Smc1β appears to be the requirement for proper telomere association to the nuclear envelope and depletion of it leads to an impairment of the structural telomeric integrity (Adelfalk et al. 2009).

Post-translational modifications (PTMs)

Post-translational modifications of cellular proteins represents a reversible way of regulating their functions. Several molecules were described to be transferred at a specific target amino acid within the protein sequence in a post-translational way (reviewed in Prabakaran et al. 2012). For instance the transfer of methyl-groups regulates proteins that are responsible for chromatin structure, important during stress response and signal transduction (Springer et al. 1979; Bedford et al. 2009). Apart from its role in chromatin organization the transfer of acetyl-groups represents an important regulator during various cellular metabolisms (Glozak et al. 2005; Zhao et al. 2013). Furthermore, the signaling of components involved in a signaling transduction cascades is dynamically regulated by phosphorylation (reviewed by Graves and Krebs 1999). Proteins can be further modified by ubiquitination which has an important role during protein degradation, DNA repair and signal transduction (Voges et al. 1999; review by Schwertman et al. 2016; May et al. 1998). Although there are several PTMs that regulate protein functions, two will be further presented.

Ubiquitin

One of the most important protein modification, known for its role in proteasomal degradation, is ubiquitin. When a protein is targeted for degradation it is ubiquitinated and thereby targeted to the 26S proteasome which catalyzed protein degradation (Voges et al. 1999). This represents one way of how proteins can be degraded, also referred as the ubiquitin-proteasome pathway. Lysine residues represents the usual targets for ubiquitination within the protein sequence whereas alternative ubiquitination sites were described in lysine less proteins (Voges et al. 1999). The ubiquitin pathway includes three enzymes, named E1, E2 and E3, that catalyze stepwise the activation and transfer of the ubiquitin to the target protein (Haas and Siepmann 1997). Ubiquitin gets activated via a catalyzed adenylation by E1 facilitating a thiol ester linkage between them. The moiety of ubiquitin is further transferred to the ubiquitin-conjugating enzyme E2. Finally E2 transfers ubiquitin to the ligase E3 which brings it to the final protein target and covalently binds it to the lysine residue. This bond can

easily be reversed by deubiquitinating enzymes (DUB) (Wilkinson 1997; Haas and Siepmann 1997; Grillari et al. 2010).

Ubiquitin itself contains seven lysine residues that can be ubiquitinated and thereby provide the formation of poly-ubiquitin chains. Ubiquitin lysine 48 (K48) represents the regularly used lysine residue which links ubiquitin to the target protein and mark it for degradation. For efficient degradation a protein needs to contain at least four ubiquitins in order to be able to bind to the degradation machinery (Grillari et al. 2010).

Besides its role in proteosomal degradation ubiquitin display several important roles in alternating protein functions. It was described to be involved in cellular senescence, telomere organization, DNA repair, signal transduction and chromatin organization (Peuscher et al. 2012; May et al. 1998; reviewed by Ulrich 2002; Schwertman et al. 2016). Here I would like to point out one particular function of ubiquitin, namely for telomere organization. The telomerase protein (TERT), which is responsible for telomere elongation, is posttranslational modified by ubiquitin to initiate its degradation. Additionally, components of the shelterin complex like TRF1 and TRF2 are ubiquitinated in order to be marked for degradation. On the other side the shelterin component TPP1 is stabilized at the telomere through the link of K63 poly-ubiquitin chains by the ubiquitin ligase RNF8 (Peuscher et al. 2012; Walker et al. 2012).

Methylation

The transfer of a methyl group is facilitated by methyltransferases, which can transfer a methyl group to an oxygen or nitrogen (O- or N-methylation) of an amino acid chain using S-adenosyl methionine (SAM) as a donor (reviewed by Roje 2006). Lysine or arginine residues represents the principal targets for methylation within the protein side chains. Protein methylation displays an important posttranslational modification for proteins that are involved in chromatin organization, stress response and cellular signaling (Bedford et al. 2009; reviewed in Biggar et al. 2014; Roje 2006). Briefly, DNA is wrapped around a multiprotein histone complex, which facilitates a 7-fold compaction of the chromatin. These histone molecules, forming the nucleosomes, can be modified by posttranslational modifications and thereby influence the chromatin compaction (Annunziato A. 2008). The methylation of lysine

residues on histones represents one of the prominent modifications within the nucleosome, regulating DNA structure and its transcription (reviewed by Zhang et al. 2012). Similar to other PTMs, the methylation of a protein is dynamically regulated through the interaction with methyltransferases (MT) and a demethylation activity. For humans 27 methyltransferases were described to target lysine residues, shortly known as KMT (reviewed by Zhang et al. 2012). Arginine methylation is in humans regulated by 9 arginine methyltransferases, members of the protein arginine methyltransferases (PRMT). The fact that a single methyl group or multi methyl groups can be formed enables a complex protein regulation via the post-translational modification (Bedford et al. 2009).

How is Smc1β regulated by PTMs during mammalian meiosis?

Here we analyze the role of two specific amino residues, lysine 361 (K361) and arginine 363 (R363), located within the amino acid side chain of Smc1β during female meiosis. In male spermatocytes K361 was observed to be ubiquitinated and R363 to be methylated (unpublished data Szydlowska-Bylicka).

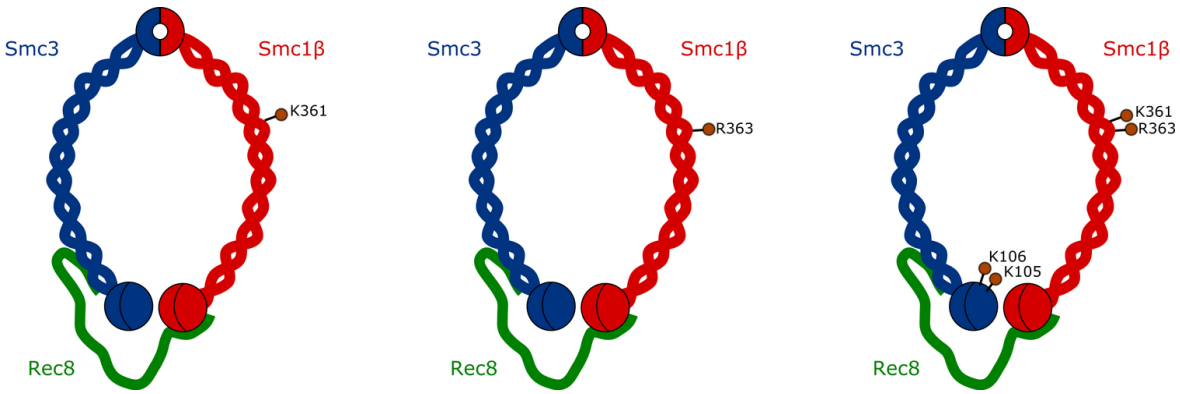

Figure 3. Schematic of meiotic cohesin complex Smc3/Smc1β/Rec8 representing the localization of post-translational modified amino residues (Courtesy of Anna Szydlowska-Bylicka, Tachibana-Konwalski laboratory)**. (A)** Cohesin complex highlighting lysine residue 361 of Smc1β as a target for ubiquitination. **(B)** Cohesin complex highlighting arginine residue 363 of Smc1β as a target for methylation**. (C)** Cohesin complex displaying K361 and R363 with close localization on Smc1β. As a control for mass spectrometry the two acetylated lysine residues on Smc3 were used (Zhang et al. 2008). (unpublished data from Anna Szydlowska-Bylicka)

Due to low material it was challenging to demonstrate by mass spectrometry whether the modifications exist in meiotic cohesin of oocytes. Nevertheless, we asked whether these particular amino residues are important for Smc1β function, which might be due to their PTMs. Therefore, we used three different mutants, each containing a replacement of the particular amino residue. By immunofluorescence we observed changes in meiotic recombination. Furthermore we show an important function of the selected amino residues for Smc1β to preserve centromeric cohesion and telomere organization. Thus our results provide molecular insight into Smc1β's role in sister chromatid cohesion, especially at the centromeric region, and the maintenance of cross overs.

Material and Methods

Mice

For our study a mixed mouse strain raised from three different strains (B6, CBA, B6129Sv) were used on the one hand as a control strain and on the other hand as a mutant strain, containing a specific replacement of a particular amino acid in Smc1β. The lysine residue 361 of Smc1β was replaced by an arginine using CRISPR/Cas9. Whereas the arginine residue 363 of Smc1β was replaced by either a glutamine or an alanine. Time-matings were performed to obtain pregnant females and the vaginal plug was checked every day in the morning to follow embryonic development directly after fertilization. The day of the plug was counted as 0.5 and at embryonic day 17.5 (E17.5) embryos were isolated. All experiments were carried out according to the guidelines of the International guiding principle for biomedical research involving animals (Council for International Organizations of Medical Science, CIOMS).

Isolation of diakinesis female oocytes

Reagents and medium

(1) M2 and M16 medium

Medium was prepared freshly every 1.5 weeks. Stocks used for medium preparation were prepared according to the protocol of Nagy et al.

(2) 10% Triton X 100 (Sigma-Aldrich, Art-Nr.: S6508-1OG, LOT# BCBH11009V) in 1x PBS

(3) 1M DTT (1,4-Dithiothreitol; Bio-Rad Laboratories, Art-Nr.: 161-0610)

(4) Acidic Tyrode (AT (pH 2.5); Sigma Aldrich, Art-Nr.: T1788 100ML)

(5) 1% Paraformaldehyde (PFA; Sigma Aldrich, Art-Nr.: 158127-500G, LOT# STBC3133V)

PFA was prepared 45min before zona removal. Heat up 32ml water (60-65°C) and pH it with 0.1M NaOH and HCl (1:100) to gain pH 9.9. 30 min before removing zona add 0.3g PFA

(6) Microscopy slides (Thermo Scientific, Superfrost Ultra Plus)

Procedure

Pair of ovaries were dissected from female mice at distinct days of age. Young females were sacrificed with an age of 10 weeks, whereas 6 months old females were used for characterization of the aged phenotype. Oocytes were transferred into oocyte collection media (M2 with IBMX). By teasing and tearing the ovary with a needle, mature oocytes were released and collected. After several washes in M2 (+IBMX) cells were transferred into droplets of oocyte culture media, M16 containing IBMX in order to prevent spontaneous meiotic maturation. Isolated WT oocytes were kept for ~30 min in the CO_2 incubator at 37°C until representative mature oocytes from KI females were isolated. After recovery of oocytes in M16 (+IBMX) at 37°C all oocytes (WT and KI) were released at the same time into the long-term culture media M16 without IBMX and incubated at 37°C until spreading. After 90min only mature oocytes undergo germinal vesicle breakdown (GVBD) and those were collected in a separate droplets of M16 (-IBMX). Five and a half hours after GVBD, oocytes were washed through droplets of M2 (-IBMX). Afterwards oocytes were transferred through acidic Tyrode (AT) droplets in order to remove their zona pellucida. After zona removal oocytes were again transferred to M2, remaining there until all oocytes processed through AT. Oocytes were then placed on an agar plate, containing 2 ml warm FBS (1:1). There they were washed three times and incubated for 14 min on the heat block (37°C). Following incubation time, 50µl supplemented PFA (1% PFA containing 15µl 10% TritonX100 (in 1x PBS) and 3µl DTT (1M)) was put in a Papen circle on microscope slides and one or two oocytes were placed into one drop with minimal FBS. Last but not least slides were then dried at RT (do not move) and afterwards frozen at -80°C.

Immunofluorescent staining of diakinesis oocytes

Reagents and medium

(1) 10% Bovine serum albumin (BSA; Sigma-Aldrich, Art-Nr.: A4503-100G, LOT# SLBJ8604V) in 1x PBS
(2) 10% Tween (Sigma Aldrich, P7949-500ML, LOT# SZBB2070V) in 1x PBS
(3) 0.08% Kodak Photo-Flo (Kodak Professional Photo-Flo 200 solution, CAT 146 4510) in 1x PBS
(4) Goat serum (Dako, Art-Nr.: X090710)
(5) Immunowash solution (2% BSA (10%), 1% Tween (10%) and 97% PBS (1x))
(6) Blocking solution (64% PBS (1x), 10% goat serum, 25% BSA (10%), 10% Tween (10%))
(7) Cleansing solution (1% Tween (10%) and 99% PBS (1x))
(8) Vectashiel mounting medium with 4,6-diamidino-2-phenylindole (DAPI, Vector Laboratories)
(9) Antibodies used:
    CREST (in house stock)
    FK2 (mono-and polyubiquinylated conjugates monoclonal antibody; Enzolifescience, BML-PW88100500)
    TRF-2 Antibody 0.1 ml Telomere marker (Novus Biological; NB 110-57130)

Immunostaining and microscopy

After several washing steps, starting with 2x 5 min in Kodak photoflo solution, followed of 2x 5 min in 1x PBS and finally 2x 5 min in immuowash solution, oocytes were incubated for at least 30 min in humidified box with 50µl blocking solution at room temperature. Afterwards, blocking solution was removed and the specific primary antibody concentration (in 10% BSA) added. Chromosomes were then incubated with primary antibody either for 1.5 hours at 37°C. Next, oocytes were washed with immunowash solution (3x 10min) and before adding the secondary antibody, oocytes were shortly washed with 1x PBS. Incubation with

secondary antibody composition (in 10% BSA) lasted for 1 hour at room temperature. After incubation and final washing steps (3x 10min cleansing solution) oocytes were mounted in Vectashield medium containing.

For kinetochore distance measurement centrosomes were identified by Crest staining (in-house stock). Oocyte isolation from 10 weeks or 6 months old female mice was performed as described. After fixation, diverse washing steps and blocking (see above), oocytes were incubated with the human anti-centromere antibody (CREST; 1:500 in block) for 1.5 hours at 37 °C, washed three times, and incubated with Alexa Fluor 594 goat anti human (1:500; Invitrogen LOT: 1117031, REF: 11014) for 1 hour at room temperature, washed again 3 times and mounted in Vectashield + DAPI. Immunofluorescence images (Z-sections) were captured with a LSM780 Axio Imager equipped with Airyscan technology – a hexagonal GaSaP detector. Using this technology for imaging our centrosomes enabled us to gain 1.7x higher resolution in order to identify centrosomes as single dots. Kinetochore distances were measured by the use of Imaris (Bitplane, version 8.0.2) core software. We used immunofluorescence images captured with a 63x/1.4 plan-apochromat Oil DIC for measuring distances. We used the following algorithm settings for measuring: spot function with different spot sizes, the estimated XY diameter was set 0.15 µm and Z diameter 0.500 µm with background subtraction. The threshold was defined to detect most of the doublets and incorrectly assigned dots were removed. The program recognizes the brightest point within one kinetochore and defines it as the center. The distance is then measured between the two centers of the kinetochore pair. If a pair of kinetochore was too close together, only one center could be determined resulting in an unresolved dataset. For accurate analyzation, unresolved kinetochores were included in all datasets.

To study the pattern of ubiquitinated proteins at the centromeric and telomeric region we co-stained for mono and polyubiquitinated conjugates (FK2), the telomere binding protein TRF2 and the centrosomes (CREST). Oocytes were isolated, as described before, from 10 weeks old female mice, fixed, washed and incubated for 1.5 hours at 37°C with the primary antibody solution, containing FK2 (1:500), TRF2 (1:700) and CREST (1:500) diluted in blocking solution. After washing, oocytes were incubated for 1 hour with the secondary antibody solution (Alexa Fluor 647 goat anti rabbit (1:500), Alexa Fluor 594 goat anti human

(1:500) and Alexa Fluor 488 goat anti mouse (1:500); in block) at room temperature, washed and mounted with Vectashield + DAPI. Serial Z-sections were captured with the inverted point laser scanning confocal microscope LSM780 Axio observer. The relative level of ubiquitinated proteins to Crest was estimated my measuring fluorescence intensity using ImageJ, with the background subtracted. For creating intensity profiles one representative chromosome was chosen for each condition and fluorescence intensity measured by ImageJ, background not subtracted.

Isolation of female meiocytes at pachytene stage

Reagents

(1) 2% PFA (pH 7.2-7.8)
Working solution (2%) was prepared from an 8% stock solution which was prepared as followed: 100ml solution: 80 ml dH_2O, 8 g PFA, 5 ml 1M Hepes HCl

(2) 10% Triton X 100 (Sigma-Aldrich, Art-Nr.: S6508-1OG, LOT# BCBH11009V) in 1x PBS

(3) 100 mM Sucrose solution (Sigma-Aldrich, Art-Nr.: S0389-500G, LOT# 011M00421V) in dH_2O

(4) Hypotonic buffer
17 mM trisodium citrate-dihydrate
50 mM sucrose
5 mM EDTA
0.5 mM DTT
30 mM Tris-HCl (pH 8.2)

(5) Microscopy slides (Thermo Scientific, Superfrost Ultra Plus)
Coated with Poly-L-lysine (0.1% (w/v) in H_2O Sigma Aldrich, P8920-100ML, LOT# SLBQ5716V)

Procedure

To gain female meiocytes at pachytene stage embryos were isolated at embryonic day 17.5 (E17.5). Embryos were removed from uterus and placenta, sacrificed by removing the head and maintained in 1xPBS on ice. Ovaries form female mouse embryos were dissected one by one, the oviduct removed and kept in 1x PBS on ice. Tail sample was obtained to confirm genotype by DNA PCR. Pairs of ovaries were then placed into a drop of hypotonic buffer on a glass slide and incubated at RT in humidified box for 20 min. Ovaries were transferred into a sucrose drop (45µl) and 21G needles were used to tease the ovary apart and to release meiocytes. The remnant chunks of the ovaries were removed and 12µl of the cell/sucrose suspension was added to 12µl of fixing solution (2% PFA and 0.2% Triton X-100) on the coated microscope slides, then incubated over night at RT. On the next day slides were air dried at room temperature and frozen at -80°C.

Immunofluorescence staining of pachytene cells

Reagents

(1) 5% BSA (Sigma-Aldrich, Art-Nr.: A4503-100G, LOT# SLBJ8604V) in 1x PBS
(2) 0.1% Triton X 100 (Sigma-Aldrich, Art-Nr.: S6508-1OG, LOT# BCBH11009V) in 1x PBS
(3) Vectashiel mounting medium with 4,6-diamidino-2-phenylindole (DAPI, Vector Laboratories)

(4) Antibodies used:
SYCP1 (Abcam, Art-Nr.: ab15090)
MLH1 (BD Bioscience, Art-Nr.: 551092)
CREST (in house stock)
SYCP3 (Abcam, Art-Nr.: ab97672)
TRF-2 Antibody 0.1 ml Telomere marker (Novus Biological; NB 110-57130)

Immunostaining and microscopy

Pachytene cells were incubated in 0.1% Triton X-100 for 10 min at room temperature and then washed 3 times with 1x PBS. Pachytene cells were incubated for at least 30 min in humidified box with 100 µl blocking solution (5% BSA in 1xPBS) at room temperature. Cells were incubated with primary antibody solution (in blocking solution) for 1.5 hours at 37°C, washed 3 times for 10 min with 0.1% Triton X 100 in PBS and then incubated for 1 hour at room temperature with the secondary antibody solution (in blocking solution) in humidified box. Lastly, oocytes were washed 3 times for 10 min with PBS-T and then mounted with Vectashield mounting medium with DAPI.

In order to analyze rate of exchange within pachytene cells we visualized MLH1 which can be seen as single foci, marking cross over formation along the synaptonemal complex, in mammalian meiosis. Pachytene cells were obtained as described above. After washing and incubating with blocking solution (see above) cells were incubated with the primary antibody solution, containing SYCP1 (1:800), MLH1 (1:50) and CREST (1:500), for 1.5 hours at 37°C. For secondary antibody solution goat anti rabbit 488 (1:500), goat anti mouse 568 (1:500) and goat anti human 647 (1:250) were used, diluted in blocking solution. Cells were washed and mounted in Vectashield containing DAPI. Immunofluorescence images (serial Z-sections) were captured by the use of an inverted point laser scanning confocal microscope LSM780 Axio observer. ImageJ was used to count MLH1 foci respectively by eye for each Z-section per cell and compiled to one dataset (number of foci / cell).

The distribution of exchange was characterized in pachytene cells by localizing MLH1 foci along the SC and in diakinesis oocytes by determining the formed chiasmata. Therefore the computer application MicroMeasure (version 3.3) was used. Further the SC and the chromosome from diakinesis oocytes were divided into three identical segments (distal / central / proximal) and MLH1 foci or visible chiasmata were assigned to the segment according their position to the centromere (Hodges et al. 2005).

Telomere structure along the synaptonemal complex was analyzed in pachytene cells by TRF2 and SYCP3 immunofluorescent staining. Pachytene cells were obtained and stained as described above. We used primary antibodies against SYCP3 (1:800), TRF2 (1:700) and

CREST (1:500) and for detection the secondary antibodies goat anti mouse 568 (1:500), goat anti rabbit 488 (1:500) and goat anti human 647 (1:250) were used. Z-sections were captured by the use of an inverted point laser scanning confocal microscope LSM780 Axio observer and immunofluorescence images analyzed by the use of ImageJ. Fluorescence intensity was measured along one representative synaptonemal complex by using ImageJ, background not subtracted.

Results

To investigate the role of particular post-translational modifications on SMC1β during the meiotic cell cycle, we analyzed female oocytes at different stages of their meiotic progression. The genome engineering technology CRISPR (Clustered regularly interspaced short palindromic repeats) / Cas9 (wildtype CRISPR-associated protein-9 nuclease from *Streptococcus pyogenes*) (Cong et al. 2013) was used to efficiently generate gene knock-in (KI) in mice by combining homologous recombination with single-stranded oligodeoxynucleotides (ssODNs) (Anna Szydlowska-Bylicka, personal communication; Yoshimi et al. 2016). Mice were obtained carrying a specific replacement for the post-translational modified amino residue within the endogenous locus of Smc1β in order to prevent its post-translational modification. Thereby the role of PTMs on SMC1β during female meiosis can be determined.

Smc1β ubiquitination at K361 is a requirement for cross-over resolution

In order to study the role of a specific lysine residue (K361) or its modification on SMC1β during meiotic progression, female mice homozygous for the replaced amino residue were used (*Smc1β* $^{K361R/K361R}$). Carrying this mutation (K361R) on Smc1β has the consequence that this particular lysine cannot be ubiquitinated anymore, and thereby its function during female meiosis can be determined.

Mice homozygous for this mutation are fertile. To further analyze the role of this post-translational modification for Smc1β functionality, oocytes in pachytene stage were isolated. To obtain female meiocytes in pachytene phase, *Smc1β* $^{K361R/K361R}$ embryos were sacrificed at embryonic day 17.5. In figure 4A a representative image of a *Mus musculus* fetus at embryonic day 17.5 is shown to illustrate its status of development (Paudyal et al. 2010). Embryonic gonads were carefully dissected from both, mutant and control embryos and no aberrant structures of the testis or ovary were observed (data not shown). Every testis isolated displayed the characteristic stripes and every ovary-structure was comparable to the WT (Fig. 4A).

To study the role of Smc1β K361 during recombination, sites of crossover were visualized by the immunostaining for MLH1, followed by counting distinct MLH1 foci along the synaptonemal complex (Fig. 4). In figure 4B the transverse filament of the synaptonemal complex can be observed by the staining of SYCP1 in WT and mutant pachytene cells. Labelling of the centromeric region (Crest) illustrates the telocentric localization of the centromeres (Silver Lee 1995) at one end of the SC. Both *Smc1β* and *Smc1β* $^{K361R/K361R}$ displayed distinct MLH1 foci along the synapsis of homologous chromosomes (Fig. 4B).

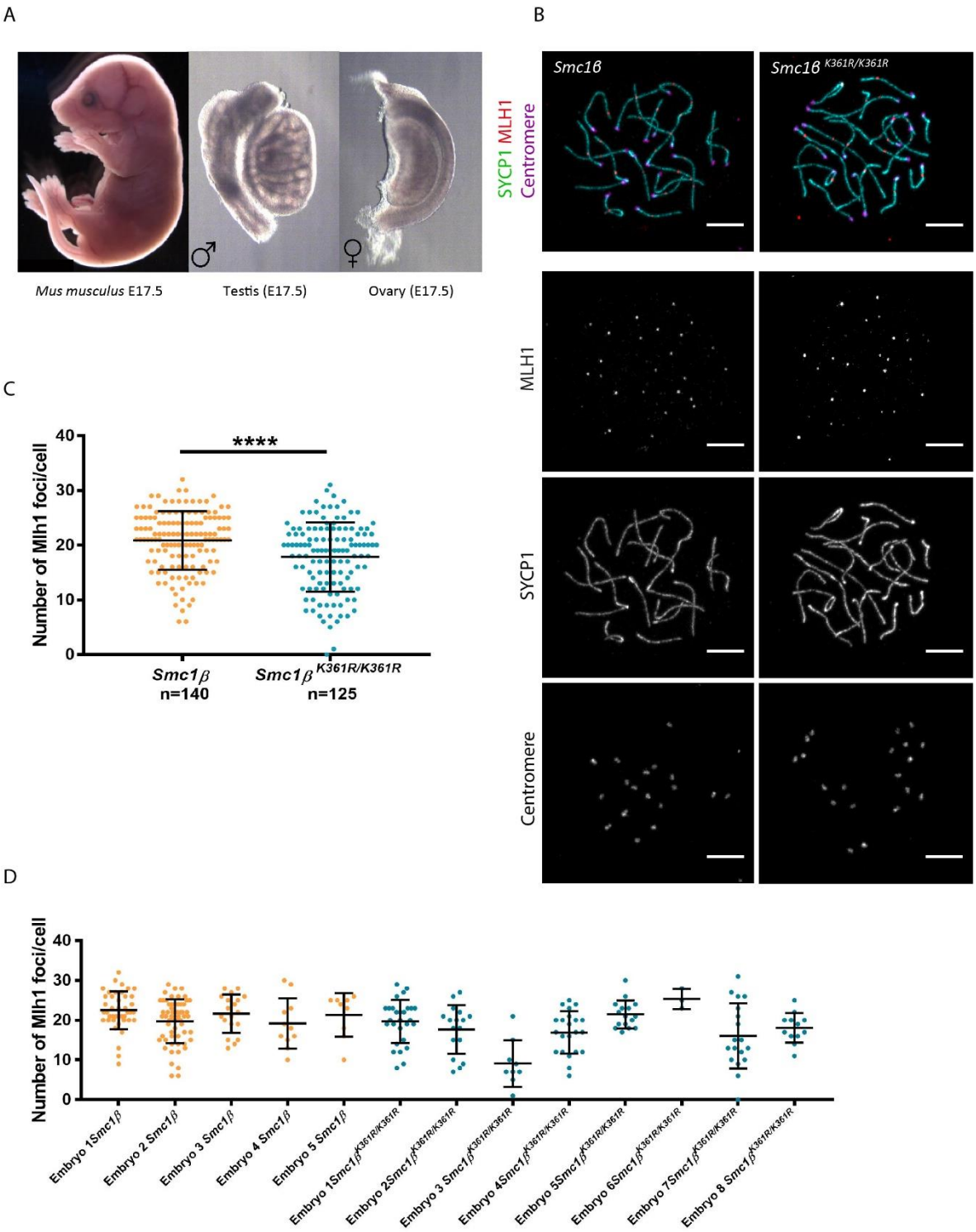

Figure 4. SMC1β K361 is important for CO resolution in mouse female meiocytes. (A) A representative image of a WT (*mus musculus*) fetus (E17.5) (modified Paudyal et al. 2010) is shown. Representative embryonic testis and ovary of wild-type B6129CBA mixed background. **(B)** Immunofluorescent staining of *Smc1β* and *Smc1β* $^{K361R/K361R}$ pachytene oocytes for SYCP1, MLH1 and Crest (staining Centromere). Scale bar = 5 µm. **(C)**

Number of MLH1 foci per cell (Pachytene stage) compiled from five *Smc1β* embryos (140 cells) and eight *Smc1β* $^{K361R/K361R}$ embryos (125 cells). The decrease is significant shown by Unpaired t-test with a p-value of <0.0001. **(D)** Data from C divided into single embryos to visualize embryo-to-embryo variability.

To determine the crossover frequency during meiotic recombination, pachytene cells displaying fully synapsed transverse filament without gaps were analyzed. In *Smc1β* pachytene oocytes, we observed 20.87 ± 0.4523 number of MLH1 foci. In *Smc1β*$^{K361R/K361R}$ pachytene oocytes, we observed 17.84 ± 0.568 number of MLH1 foci, suggesting that crossover maturation is less efficient. Moreover, in wild-type pachytene oocytes, every SC displayed at least one MLH1 focus, whereas this was not observed in *Smc1β*$^{K361R/K361R}$ oocytes. The mean number of foci was reduced from 20.87 in wild-type to 17.84 in *Smc1β*$^{K361R/K361R}$ (reduced by 15%). We note that the detection of MLH1 foci varies between embryos, implying that underscoring due to technical reason could lead to a lower number of MLH1 foci. These results show a decreased frequency of exchange in *Smc1β*$^{K361R/K361R}$, suggesting either an altered maturation of recombination or a delayed progression of recombination due to the replacement of a single amino residue.

Smc1β ubiquitination of K361 is important for cross-over maintenance

We next tested whether Smc1β K361 is important for crossover distribution. It was previously shown that SMC1β is involved in crossover maintenance during female meiosis (Hodges et al. 2005). Therefore we compared the localization of MLH1 foci in pachytene oocytes to sites of chiasmata in diakinesis oocytes. To determine the localization of MLH1 foci relative to the centromere, the length of every measured SC was divided into three identical parts (illustrated in figure 5A). According to the measured distance, MLH1 foci were categorized as a distal, central or proximal foci in relation to the centromere. When two MLH1 foci were present their positions were categorized similar to the single foci (one representative variant, with MLH1 foci distal and proximal, is illustrated in Fig. 5A). To compare the distribution of CO in a pachytene cell with the followed chiasmata in a diakinesis oocyte, sites of chiasma were determined in relation to the centromere along the chromosome axis of diakinesis oocytes. Categories were chosen the same way as for the MLH1 localization (distal / central / proximal) (Fig. 5A).

The incidence of single MLH1 foci in *Smc1β*$^{K361R/K361R}$ was comparable to *Smc1β* pachytene cells (Fig. 5B). About 70% of each *Smc1β* and *Smc1β*$^{K361R/K361R}$ SC axis contained only one MLH1 foci. Accordingly the frequency of 2 MLH1 foci per SC did not change due to the mutation (Fig. 5B and Table 1). Although we observed a reduced level of exchange sites in *Smc1β*$^{K361R/K361R}$ (Fig. 4), the mutation had no effect on the overall number of single or double MLH1 foci along the SC.

In control and mutant oocytes most of the single MLH1 foci were observed in the middle of the SC, some at the distal end and only few in close proximity to the centromere (Fig. 5B). To test whether the distribution of mature CO detected in pachytene cells correspond to chiasmata placement in diakinesis we examined chiasma localization in meiosis I chromosome spreads. In *Smc1β* oocytes the placement of chiamata was minimally changed from less proximal to more central distributed compared to the corresponding CO in pachytene cells (Fig. 5C). This result suggests an inhibition of crossovers near the centromeric region. In *Smc1β*$^{K361R/K361R}$ the CO distribution was skewed towards the central and distal region of chromosomes in diakinesis oocytes (Table 1; Fig. 5C). Whereas the proximal placed COs were less observed in diakinesis oocytes and only half of the double COs observed in pachytene cells were present as chiasmata in diakinesis oocytes (Table 1). This results indicate problems during crossover maintenance arising during the transition of pachytene to diakinesis in mutant oocytes.

In both *Smc1β* and *Smc1β*$^{K361R/K361R}$ oocytes more than half of double COs were located distal and proximal to the centromere (Fig. 5D). The fact that in *Smc1β* oocytes the distribution of two cross over events is skewed towards proximal / distal in diakinesis oocytes (Fig. 5E), suggests a dynamic regulation by crossover interference for preventing exchanges in close proximity (Bishop and Zickler 2004). In *Smc1β*$^{K361R/K361R}$ oocytes the placement of chiasmata localized proximal / distal to the centromere were reduced (Fig. 5E) compared to the corresponding CO in pachytene cells (Fig. 5D). Accordingly more proximal / central chiasmata were observed (Fig. 5E).

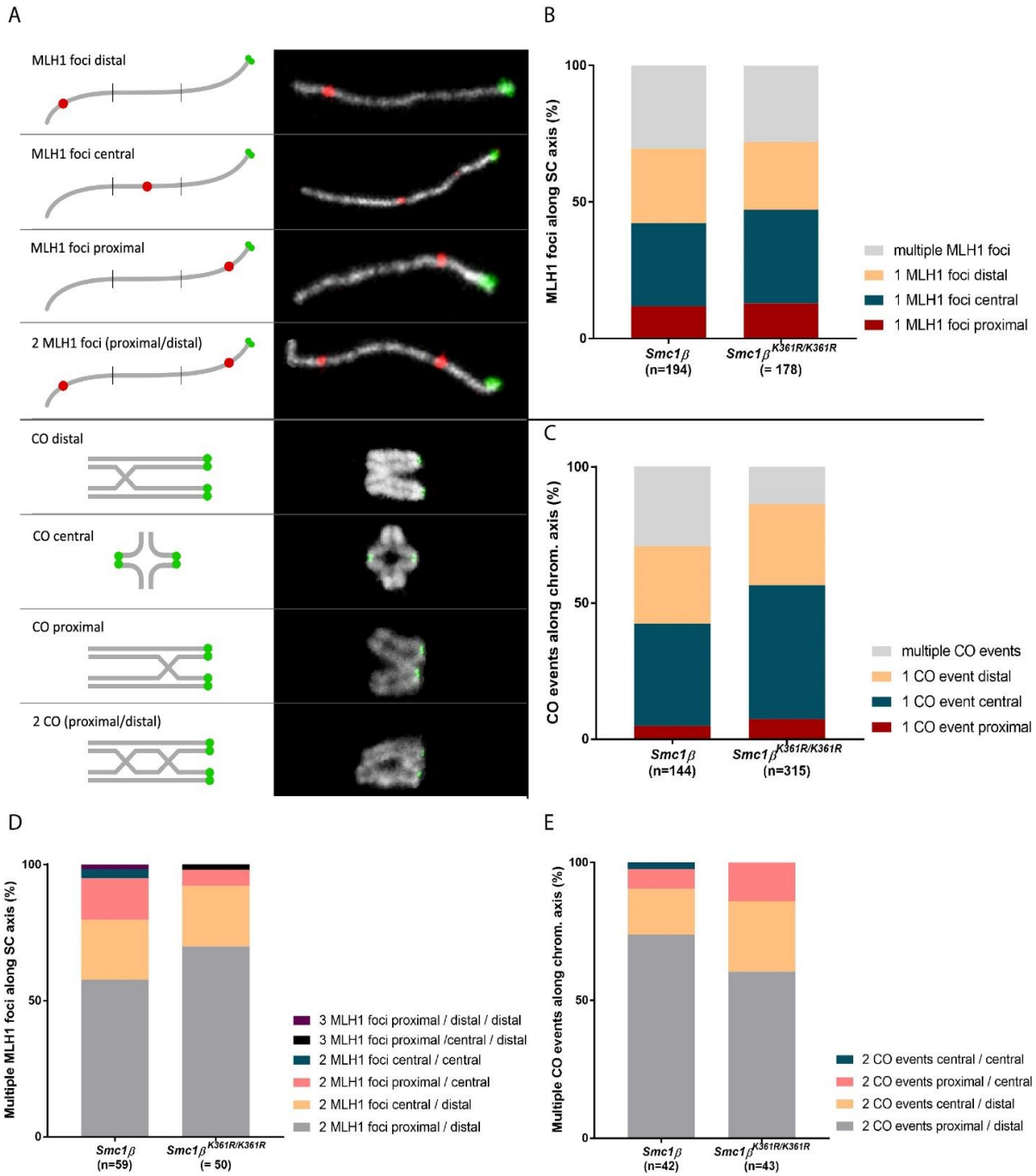

Figure 5. SMC1β K361 promotes maintenance of cross over sites. (A) Left panel shows the schematic of the determination CO-designated sites and resulting chiasmata. Right panel illustrates Examples for each category, showing MLH1 foci in red, SC and chromosome axis in gray and centromere in green. **(B)** Distribution of single and double MLH1 foci along the SC axis. **(C)** Localization of CO events along the chromosome axis. **(D)** Multiple MLH1 foci along the SC axis. **(E)** Localization of two CO events along the chromosome axis.

Table 1 Frequency of MLH1 foci in Pachytene cells compared to chiasmata formation in Diakinesis.

	Placement 1 MLH1 foci / 1 chiasmata (%)[b]			Multiple MLH1 foci / CO (%)[c]
Smc1β	proximal	central	distal	
Pachytene (n=10)[a]	11,86	30,41	27,32	30,41
Diakinesis (n=10)	4,86	37,50	28,47	29,17
Smc1β$^{K361R/K361R}$				
Pachytene (n=10)	12,92	34,27	24,72	28,09
Diakinesis (n=22)	7,30	49,21	29,84	13,65

[a] Number of cells analyzed [b]Distribution of one MLH1 foci (in pachytene cells) along SC versus one chiasmata (in diakinesis cells) along chromosome axis. In *Smc1β$^{K361R/K361R}$* the central exchanges and the frequency of 2 MLH1 foci[c] are skewed.

These results show a quite different trend of the maintenance of double CO, when *Smc1β$^{K361R/K361R}$* is compared to *Smc1β*. In the wild type the number of double CO in pachytene cells correspond to the number of chiasmata visible in metaphase I, whereas the position of it seems more or less variable. This indicates a dynamic movement of double crossovers in order to inhibit CO that are too close. The result that only half of the double COs observed in *Smc1β$^{K361R/K361R}$* pachytene cells were also present as chiasmata in diakinesis indicates that only half of the CO maintained. This suggests a slipping off of distal CO during the transition of pachytene to diakinesis which gets even more obvious considering the increase of central CO and the reduction of double proximal / distal CO events.

Aberrant telomere structures in absence of Smc1β ubiquitination at K361

Based on the observation that in full *Smc1β* knock-out meiocytes the telomere structure is affected (Adelfalk et al. 2009), we asked whether ubiquitination at K361 on Smc1β is necessary for telomere organization. In WT meiocytes, telomere ends attach to the nuclear envelope in order to be brought together forming a bouquet. This bouquet formation is important for bringing homologous chromosomes into close proximity to further establish synapsis between the homologs (reviewed by Scherthan 2007). In *Smc1β$^{-/-}$* the telomere organization is impaired resulting in various visible phenotypes during the leptotene to pachytene transition (Adelfalk et al. 2009). To study the telomere organization in our mouse models we used an antibody against the telomere binding protein TRF2. In a WT cell TRF2

binds to the repetitive sequence located at both ends of the chromosomes in order to stabilize chromosome ends and prevent telomere end fusion (Bilaud et al. 1997; Van Steensel et al. 1998; Okamoto et al. 2013). In our study we had a closer look at the meiotic pachytene stage and in order to visualize the localization of TRF2 on chromosome ends we stained for the axial element SYCP3. Similar to the literature our WT cells displayed two specific TRF2 foci on both ends of the SC, one very close to the centromeric region (Scherthan et al. 2000). Figure 6A illustrates a representative *Smc1β* pachytene cell, stained for SYCP3/TRF2/Centromere. The synaptonemal complex is assembled and no separated axial elements can be observed. The close localization of one telomere end to the centromeric region represents one characteristic described for mouse chromosomes, containing only telocentric chromosomes (Fig. 6A).

A detailed view of the SC/telomere/centromere organization offers the measured intensity profile of a selected synaptonemal complex in *Smc1β*. The measured profile displayed two intensities for the telomere protein TRF2, each co-localizing at one end with the axial element. One peak for the centromeric region can be observed at the beginning of the intensity profile. The telocentric localization of the centromere is visible in the profile as an overlapping centromeric peak with one telomere peak. In $Smc1\beta^{K361R/K361R}$ pachytene cells we were able to observe infrequent axial elements without co-localization of TRF2 signals. One cell was selected displaying a representative mutant pachytene cell (Fig. 6B). Within the cell the axial element is visibly formed and also the telocentric localization of the centromere can be observed. For further analyzation we picked one axial element that showed two TRF2 signals at both ends of the SC, visibly co-localizing with it. Starting with the telocentric end, a slight shift of the TRF2 intensity away from the SC can be observed. Same is also true for the other telomeric region. Whereas in the WT the TRF2 signal completely overlapped with the SC, the mutant displayed a shift away from it. The fact that we observed cells containing complete disconnected telomere ends, suggest an altered telomere organization due to the replacement of one particular amino residue in Smc1β.

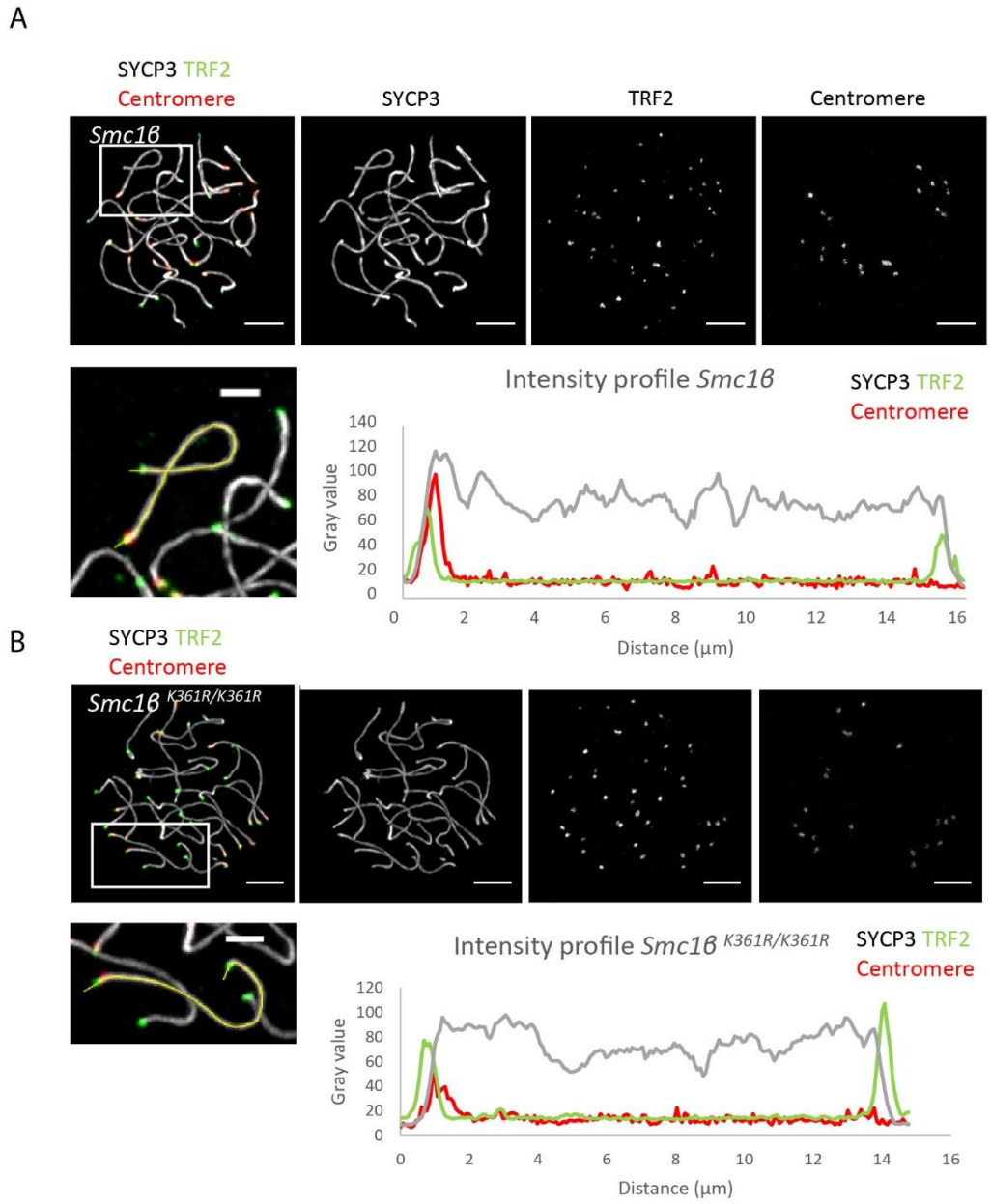

Figure 6. Localization of the telomere associated protein TRF2 at the synaptonemal complex. (A) Representative WT pachytene cell immunostained for the axial element component SYCP3, the telomere protein TRF2 and for the centromeric region via Crest; Scale bar = 5µm. A full synapsed SC with centromeres located at one telomere end. Two distinct TRF2 foci can be observed on both ends of the SC. One SC of the representative cell was selected (magnified image; Scale bar = 2 µm) to show a detailed representation of the structural organization of the telocentric SC in an intensity profile. The profile was measured along the depicted SC (yellow line) representing in gray the intensity measurement for SYCP3, in green for TRF2 and in red for Crest. A co-localization of the two TRF2 foci with the SC can be observed. The telocentric organization is visible by an overlapping centromere and TRF2 peak. **(B)** An exemplar of a *Smc1β* $^{K361R/K361R}$ pachytene cell representing the axial element (SYCP3), telomere ends (TRF2) and the centromere (Crest). TRF2 foci are visible on ends of SYCP3 elements each containing one centromere. The magnified image shows a SC complex with

telomere localization. The intensity profile, measured along the yellow line, uncovers the separated TRF2 signal from SYCP3.

Due to our observations that the telomere structures might be impaired in mutant cells, we asked whether the mutation has a negative effect on the bouquet formation, formed at the zygotene to pachytene transition (reviewed by Scherthan 2007). We used the pool of cells isolated E 17.5 to search for pre-pachytene cells. In the WT and in our mutant we were able to identify some cells displaying early meiotic stages and for both, cells were observed forming a bouquet. Figure 7A illustrates a representative WT cell displaying a bouquet formation. The bouquet is formed due to an assembly of telomere ends at one side of the nuclear envelope. Within $Smc1\beta^{K361R/K361R}$ cells were found containing assembled telomere ends (Fig. 7B). When we looked closer at the telomere structure within the bouquet aberrant structures could be observed in some cases. Two examples of aberrant TRF2 structures are shown in figure 7B and 7C. In the cell represented in figure 7B, five axial elements formed with their telocentric telomere ends a bouquet. Within this assembly the reciprocal telomere attachment seems to be impaired, displaying a stretched TRF2 structure for one telomere end (magnified image, white arrow). The example illustrated in figure 7C displayed two cells located close together. One cell displayed a bouquet-like structure, whereas the other entered already pachytene stage. Even though cells were found in $Smc1\beta^{K361R/K361R}$ displaying completely normal bouquet structures, we were able to observe aberrant structures in some cases. One phenotypic alteration can be observed within the cell displaying the bouquet-like structure in figure 7B. Within the upper magnified image (Fig. 7B) an altered bouquet-like structure can be observed. The telomere ends do not form a tight association like in the control cell, it seems like they lost their cohesion and are about to fall apart (white arrowhead). Furthermore some of the telomeres seem to stay in contact with another telomere but due to the loss of cohesion this results in additional TRF2 signal between those stretched telomere pairs. The second cell represented in figure 7B displayed completely synapsed synaptonemal complexes in pachytene. However the staining for TRF2 displayed an additional telomere structure formed between three telomeric ends (Fig. 7C, magnified image yellow arrowhead). These structures were also found in SMC1β full knock-out, characterized as telomere bridges, by Adelfalk and

her colleagues (Adelfalk et al. 2009). These results suggests a role of SMC1β for telomere organization which further supports the idea of cohesin complexes to be required for preserving telomere architecture (Adelfalk et al. 2009; Scherthan 2007).

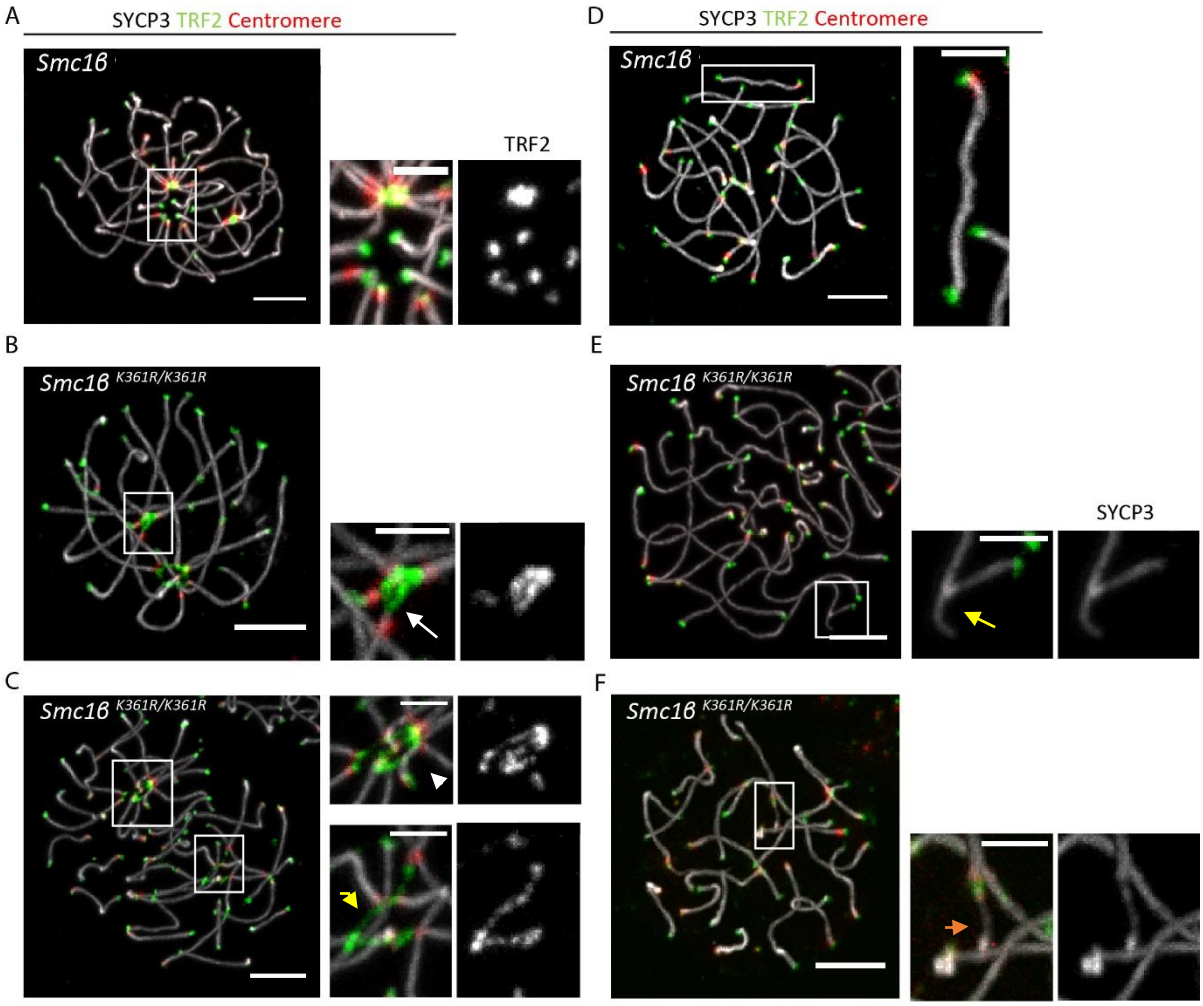

Figure 7. Aberrant telomere and SYCP3 structures in *Smc1β*$^{K361R/K361R}$ meiocytes. (A) Representative image of a WT cell displaying the bouquet formation. Telomeres are visualized by TRF2 staining on the SC via SYCP3 staining. The centromere is labeled by Crest displaying telocentric localization. Within the magnified image the bouquet can be observed. **(B)** Mutant cell containing a stretched telomere within a telomere assembly. **(C)** Two cells are illustrated, one representing a bouquet-like structure with loss of telomere cohesion. The second cell, entered pachytene stage, displays a telomere bridge. **(D)** A representative WT pachytene cell is shown with completely synapsed axial elements visible via SYCP3 staining. One particular SC can be observed in a magnified image, displaying two TRF2 signals and one telocentric centromere. **(E)** A representative mutant pachytene cell displaying for one SC a separated axial element (magnified image). **(F)** A representative mutant pachytene cell containing for one SC an additional SYCP3 structure (magnified image).

Every *Smc1β* pachytene cell is characterized by a fully synapsed axial element via the central element, which holds homologous chromosomes together in order to facilitate recombination. In figure 7D a representative WT pachytene cell is stained for the axial elements via SYCP3, the telomeres by labelling TRF2 and the centromere to locate the telocentric end. In $Smc1\beta^{K361R/K361R}$ pachytene cells, most of the SC consists of two fully synapsed axial elements. Additionally variable SYCP3 structures were observed. Two exemplary structures are illustrated in figure 7E and 7F showing additional SYCP3 structures along the full synapsed SC. The first selected cell represents a pachytene cell were the two axial elements are fully synapsed. However for one particular SC an additional SYCP3 structure was arising at one telomere end. We are confident to believe that this is not due to an unfinished synapsis, since no TRF2 signal is visible at the end of this structure (figure 7E, magnified image yellow arrow). The second selected cell represents again the meiotic pachytene stage with a synapsed SC and a normal TRF2 pattern (Fig. 7F). A closer look at one particular SC uncovered an SYCP3 extension on the telocentric end (Fig. 7A, magnified image orange arrowhead). These results, indicating an unfrequently aberrant assembly of the axial element component SYCP3 due to the mutation of a single amino residue in Smc1β, suggests that SMC1β is not an essential requirement for SC formation but can affect the structure of the axial elements.

Smc1β methylation at R363 is important for cross-over resolution

The second post-translational modification analyzed in this thesis involves an arginine at position 363 (R363) on Smc1β, which was identified to be methylated in male spermatocytes (unpublished data Szydlowska-Bylicka). Similar to the first analyzed post-translational modification K361, mice containing a specific mutation for R363 were used to study the role of this particular methylation mark. This time mice with two different genotypes were used $Smc1\beta^{R363Q/R363Q}$ and $Smc1\beta^{R363A/R363A}$. For both genotypes homozygous mice were fertile.

First we asked whether the methylation on R363 is important for recombination and CO resolution. Therefor $Smc1\beta^{R363Q/R363Q}$ and $Smc1\beta^{R363A/R363A}$ meiocytes were analyzed at pachytene stage for CO-designated sites. Female pachytene cells were isolated from ovaries at embryonic day 17.5. To visualize sites for recombination along the synaptonemal complex,

cells were labelled for the transverse filament (SYCP1), recombination sites (MLH1) and for the centromeric region (Crest).

When comparing WT pachytene cells with cells isolated of *Smc1β*$^{R363Q/R363Q}$ ovaries, a synapsed telocentric SC with distinct MLH1 foci distributed along the axial element can be observed in both cases (Fig. 8B).

To further assess the importance of methylated R363 for CO formation, visible MLH1 foci were counted along the synaptonemal complex. Only real pachytene cells, characterized by a fully synapsed transverse filament without gaps, of three *Smc1β* embryos were compared to cells of three *Smc1β* $^{R363Q/R363Q}$ embryos. In mutant pachytene cells, the number of MLH1 foci distributed along the SC, was significantly reduced (12%) compared to the WT. In *Smc1β* pachytene oocytes, we observed 21.48 ± 0.4417 number of MLH1 foci. In *Smc1β*$^{R363Q/R363Q}$ pachytene oocytes, we observed 18.95 ± 0.9476 number of MLH1 foci, suggesting that crossover maturation is less efficient (Fig. 8A). This indicates a role of Smc1β R363 during the progression of recombination.

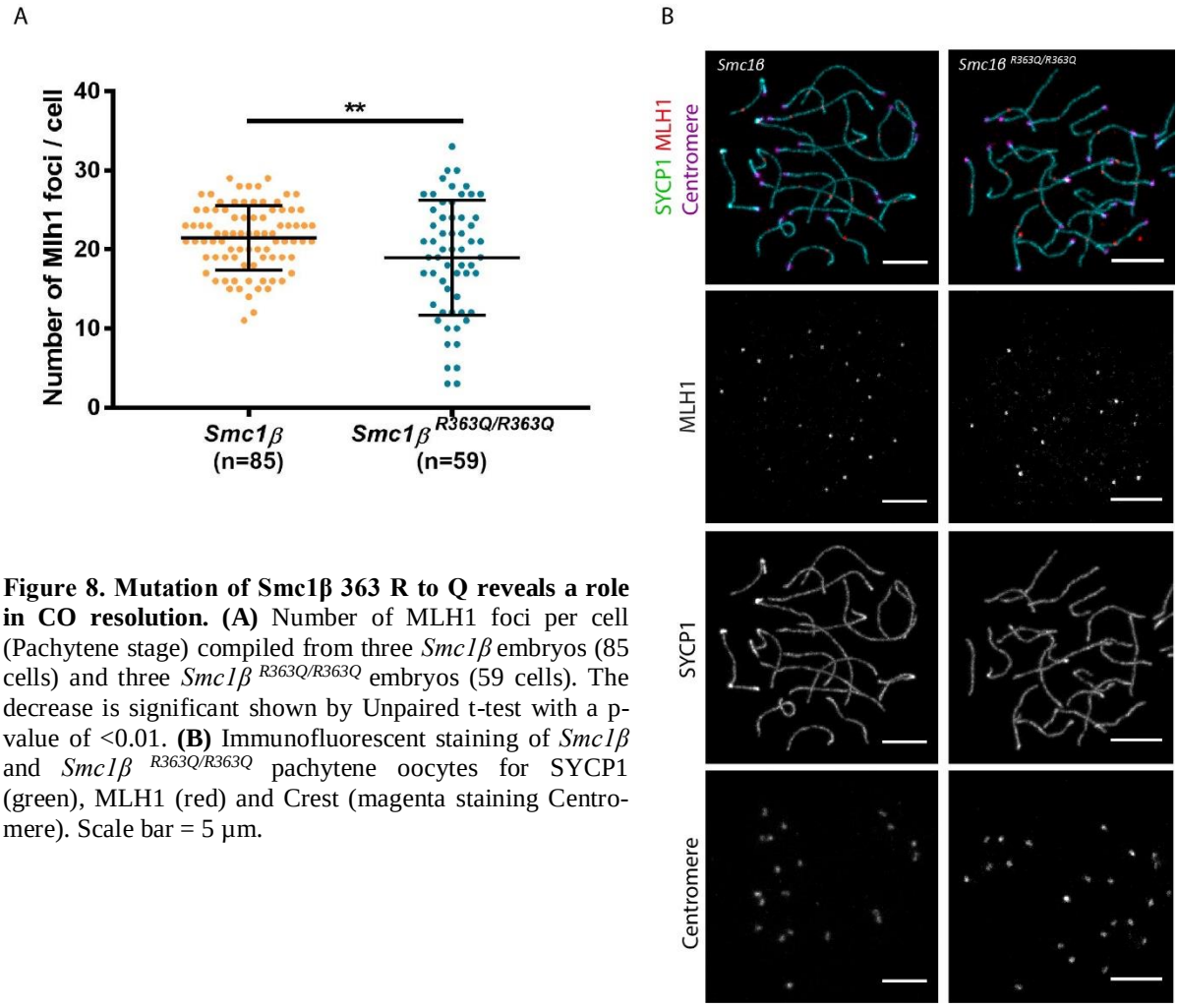

Figure 8. Mutation of Smc1β 363 R to Q reveals a role in CO resolution. (A) Number of MLH1 foci per cell (Pachytene stage) compiled from three *Smc1β* embryos (85 cells) and three *Smc1β* $^{R363Q/R363Q}$ embryos (59 cells). The decrease is significant shown by Unpaired t-test with a p-value of <0.01. **(B)** Immunofluorescent staining of *Smc1β* and *Smc1β* $^{R363Q/R363Q}$ pachytene oocytes for SYCP1 (green), MLH1 (red) and Crest (magenta staining Centromere). Scale bar = 5 µm.

In figure 9B a representative image of a *Smc1β* pachytene cell can be observed. The control pachytene cells displayed a fully synapsed transverse filament, illustrated by SYCP1, with a centromere localized at one telomere end. Within the WT variable numbers of MLH1 foci can be observed along the SC. In *Smc1β*$^{R363A/R363A}$ pachytene cells, the formation of a fully synapsed SC is not impaired, representing a normal SYCP1 assembly. Furthermore variable amounts of MLH1 foci can be observed within the mutant pachytene cells suggesting a nonessential function of this posttranslational modification for recombination (Fig. 9B).

Although every *Smc1β*$^{R363A/R363A}$ pachytene cell contained distinct MLH1 foci, the number of viable CO sites were quite different compared to *Smc1β.* MLH1 foci were counted along fully synapsed SC in 53 WT cells and compared to numbers counted in 82 mutant pachytene cells, illustrated in figure 9A. In *Smc1β* every SC contained at least one MLH1 foci

(21.17 ± 0.6106). By contrast, in *Smc1β*$^{R363A/R363A}$ pachytene oocytes, we observed 17.05 ± 0.5825 number of MLH1 foci, displaying a reduction by 19 % relative to the WT (Fig. 9A).

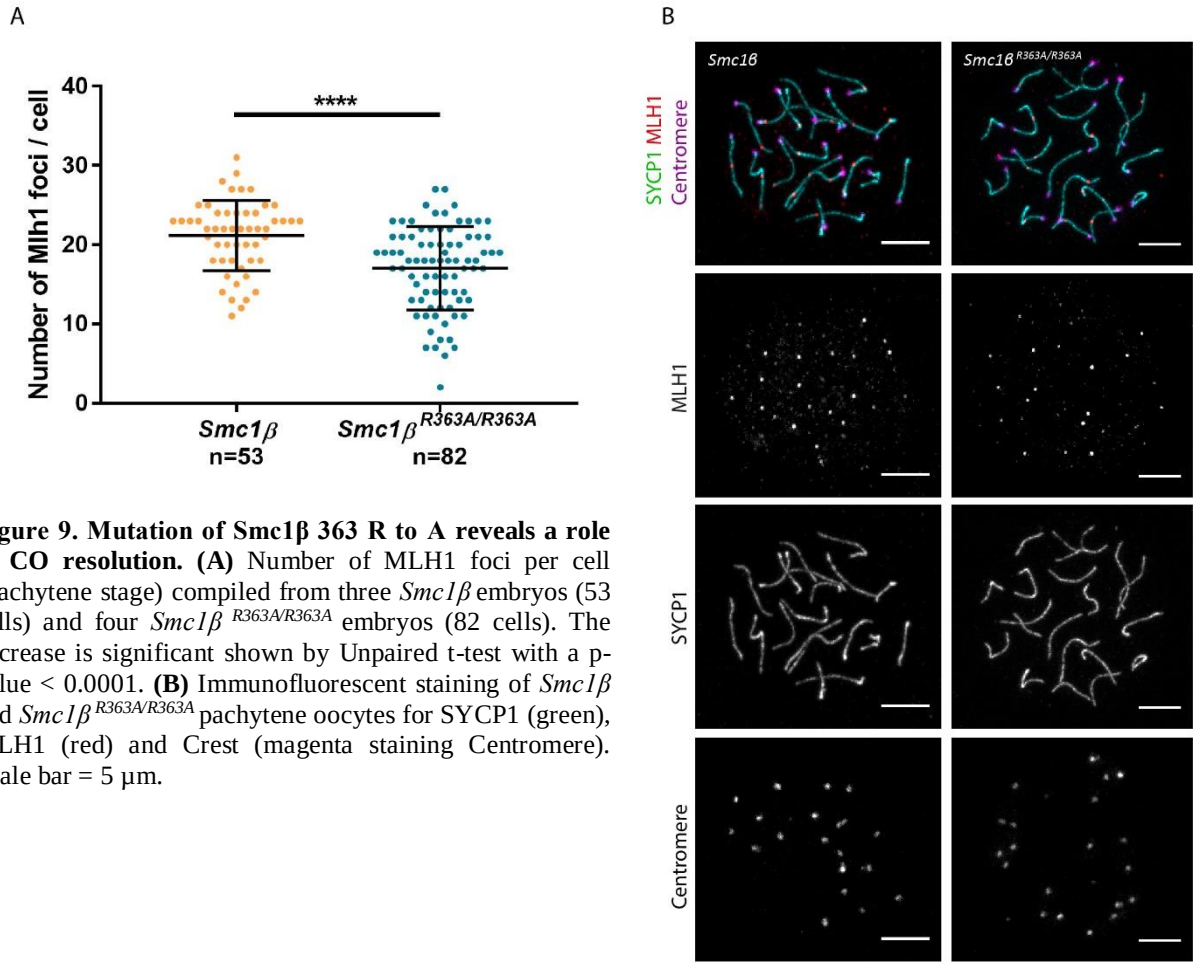

Figure 9. Mutation of Smc1β 363 R to A reveals a role in CO resolution. (A) Number of MLH1 foci per cell (Pachytene stage) compiled from three *Smc1β* embryos (53 cells) and four *Smc1β* $^{R363A/R363A}$ embryos (82 cells). The decrease is significant shown by Unpaired t-test with a p-value < 0.0001. **(B)** Immunofluorescent staining of *Smc1β* and *Smc1β* $^{R363A/R363A}$ pachytene oocytes for SYCP1 (green), MLH1 (red) and Crest (magenta staining Centromere). Scale bar = 5 µm.

Regardless of the modification, both mutants *Smc1β*$^{R363Q/R363Q}$ and *Smc1β*$^{R363A/R363A}$ displayed a reduced level of MLH1 foci, suggesting an important role of this particular arginine residue at position 363 for the maturation of CO in a WT pachytene cell. However we noted a discrepancy between the level of MLH1 foci in *Smc1β*$^{R363Q/R363Q}$ and *Smc1β*$^{R363A/R363A}$ relative to the WT. On the one hand, changing the arginine residue into a glutamine resulted in a MLH1 reduction of 12% compared to the WT. On the other hand, changing it into an alanine leads to a greater reduction of the MLH1 level (19 %) relative to the WT. The different levels of MLH1 foci within the mutants might be a consequence of changing the arginine into differing amino acids.

Arginine is a member of charged amino acids, glutamine represents a polar structure and alanine is non-polar (Müller-Esterl et al. 2011). The charge of arginine might represent an important requirement for conformational changes which is lost when arginine is replaced by alanine. A stronger phenotype when arginine is replaced by alanine could be either due to the importance of the charge or due to a conformational change caused by the small structure of alanine.

Reduced level of ubiquitinated proteins in *Smc1β*$^{K361R/K361R}$ oocytes

Next we asked whether changing one particular amino acid of a protein, which was shown to be ubiquitinated in spermatocytes, can affect the overall level of ubiquitinated proteins in female oocytes. Oocytes isolated from *Smc1β* females displayed a distinct pattern for ubiquitinated proteins in metaphase I. Figure 10A illustrates a representative image of a WT oocyte in diakinesis stage, representing highly condensed telocentric chromosomes forming visible chiasmata. In metaphase I ubiquitinated proteins can be visualized by immunostaining along every WT chromosome. With a broad distribution, ubiquitinated proteins can be observed along the chromosome axis and with an increased amount at the centromeric and telomeric region (see orange square fig. 10A). Similar to *Smc1β*, chromosomes of *Smc1β*$^{K361R/K361R}$ can be detected in metaphase I in a condensed form displaying chiasmata. Also in the mutant ubiquitinated proteins can be detected. However the immunostaining illustrates less ubiquitinated proteins along the chromosome when K361 is mutated (see blue square fig. 10A).

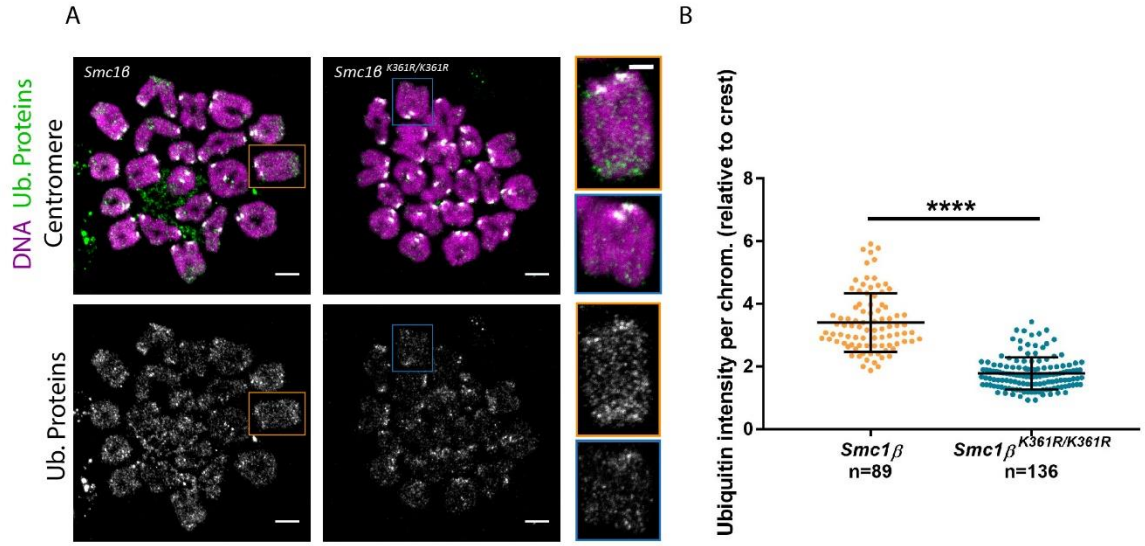

Figure 10. Ubiquitin quantification by immunofluorescent staining of *Smc1β* and *Smc1β*$^{K361R/K361R}$ Metaphase I oocytes. (A) Exemplary images of Diakinesis chromosome spreads in *Smc1β* and *Smc1β*$^{K361R/K361R}$ immunostained for ubiquitinated proteins (FK2), centromere (crest) and DNA (Dapi); Scale bar = 5µm. A magnified image of a WT chromosome is illustrated in an orange square. The blue square contains a magnified chromosome of *Smc1β*$^{K361R/K361R}$. Scale bar for magnification = 2 µm. **(B)** Quantification of total ubiquitin level per chromosome relative to crest signal. Data was collected from 89 chromosomes for *Smc1β* and 136 chromosomes for *Smc1β*$^{K361R/K361R}$ resulting in a significant difference of ubiquitinated proteins in *Smc1β*$^{K361R/K361R}$ (Unpaired t-test p-value <0,0001).

To confirm our observation that *Smc1β*$^{K361R/K361R}$ display less ubiquitinated proteins the overall level of ubiquitinated proteins was analyzed. The total intensity of ubiquitin, measured for every single chromosome, showed a significant decrease within the mutant relative to the WT. Mutating only one lysine residue resulted in a 2-fold reduction of global ubiquitin levels in *Smc1β*$^{K361R/K361R}$ (Fig. 10B).

The fact that we observed an increase of ubiquitinated proteins at the centromeric and telomeric region forced us to analyze this coincidence in a more detailed manner. To gain a more specific insight into the organization of ubiquitinated molecules along the chromosomal axis, intensity profiles were compiled. For both, *Smc1β* and *Smc1β*$^{K361R/K361R}$, chromosomes in metaphase I were immunostained for a specific telomere protein (TRF2) to mark the telomeric region. Additionally, labelling ubiquitinated proteins and the centromeric region enabled us to create an intensity profile for all three conditions. Intensity profiles for one representative chromosome per cell were collected. Figure 11A illustrates one representa-

tive measurement for *Smc1β* and *Smc1β*$^{K361R/K361R}$, where the measured chromosome is magnified in an orange square for the WT and in a blue square for the mutant. The yellow line in the magnified images represents the measured area (Fig. 11A) and the corresponding profiles are illustrated below (Fig. 11B).

In *Smc1β* an area with a length of 9 µm was measured, depicted along one sister chromatid. The centromeric region can be observed as one characteristic peak at the beginning of the intensity profile. Looking at the profile of ubiquitinated proteins along the depicted area an alternating curve can be observed with a co-localization at the centromeric region (Fig. 11B left). The intensity profile for the telomere protein TRF2 reflects the observation seen in the immunostaining. TRF2 proteins localize at both ends of the sister chromatid, visible as two peaks in the intensity profile. Blotting the same alternating curve of ubiquitinated proteins against the telomere profile a co-localization can be observed. Despite the variable pattern of ubiquitinated proteins along this particular sister chromatid, there were more ubiquitinated proteins localizing to the centromeric and telomeric regions in *Smc1β*.

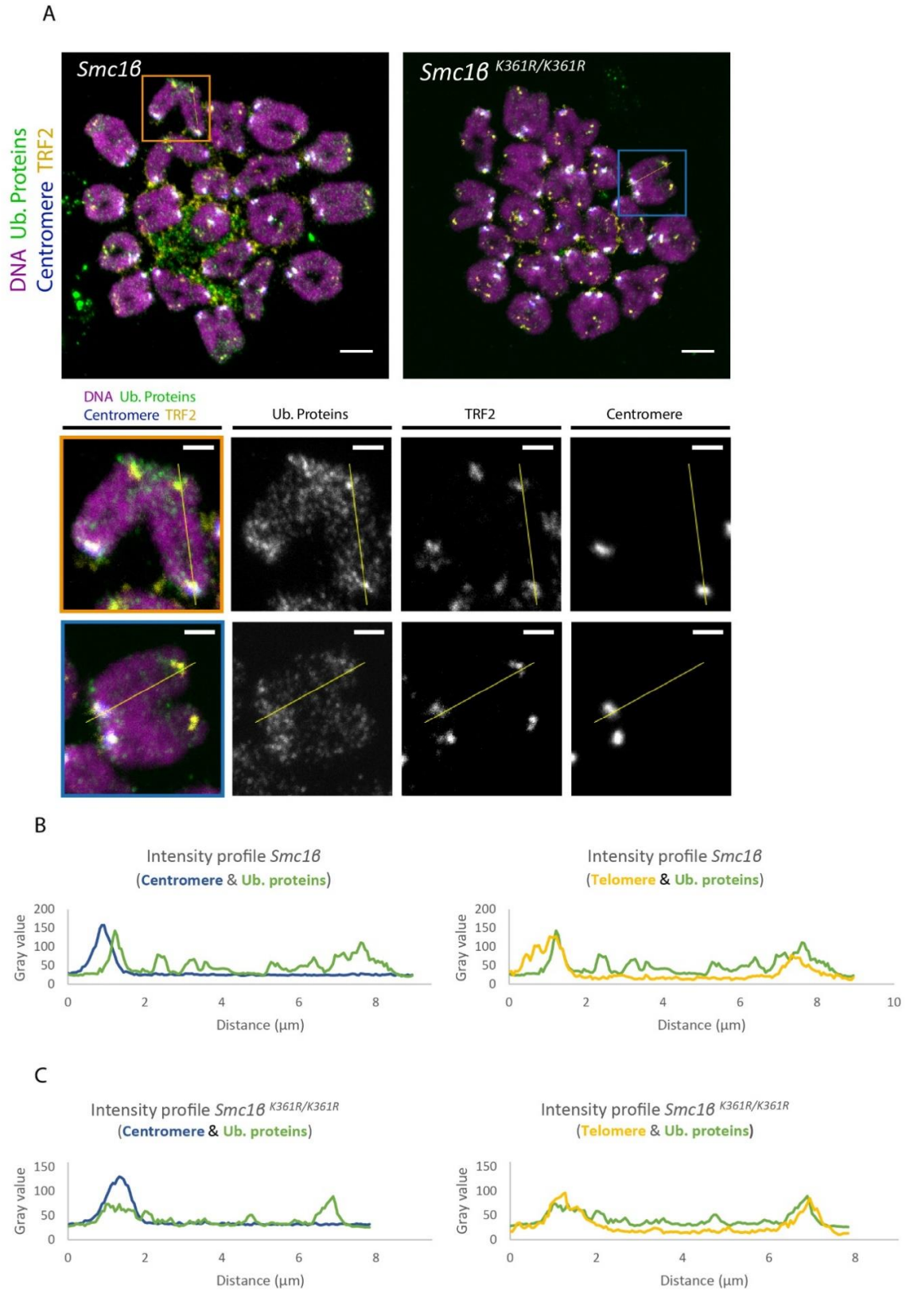
A
Smc1β
Smc1β K361R/K361R
DNA Ub. Proteins
Centromere TRF2
DNA Ub. Proteins
Centromere TRF2
Ub. Proteins
TRF2
Centromere
B
Intensity profile Smc1β
(Centromere & Ub. proteins)
Gray value
Distance (μm)
Intensity profile Smc1β
(Telomere & Ub. proteins)
Gray value
Distance (μm)
C
Intensity profile Smc1β K361R/K361R
(Centromere & Ub. proteins)
Gray value
Distance (μm)
Intensity profile Smc1β K361R/K361R
(Telomere & Ub. proteins)
Gray value
Distance (μm)

Figure 11. Localization of ubiquitinated proteins to centromeric and telomeric regions. (A) Representative images of *Smc1β* and *Smc1β*$^{K361R/K361R}$ oocytes in Metaphase I immunostained for TRF2, ubiquitinated proteins (FK2), centromere (Crest) and DNA (Dapi); Scale bar = 5 µm. WT Chromosome used for intensity measurement is represented with higher magnification in the orange square. The mutant chromosome is magnified in the blue square; scale bar = 2µm. **(B)** Intensity profiles of the *Smc1β* representative chromosome (depicted line ~ 9µm). Measurement for centromere (blue) & ubiquitinated proteins (green) are shown in the left diagram. Comparison telomere (yellow) & ubiquitinated proteins (green) is illustrated in the right diagram. **(C)** Intensity profiles of the *Smc1β*$^{K361R/K361R}$ representative chromosome (depicted line ~7.8 µm). Left diagram: measurement centromere & ub. proteins; Right diagram: measurement telomere & ub. proteins.

In *Smc1β*$^{K361R/K361R}$ a line with a length of 7.8 µm was drawn along one particular sister chromatid and used for the representative intensity profile. In the left diagram of figure 10C the profile measured for Crest (labelling for the centromeric region) is compared to the profile measured for ubiquitinated proteins. Similar to the WT the centromere is visible in the *Smc1β*$^{K361R/K361R}$ intensity profile as a single peak. As expected the reduced level of ubiquitinated proteins can be also observed within the measured profile. Whereas in the WT ubiquitinated proteins can be observed along the body of the sister chromatid, little or no signal for ubiquitinated proteins was detectable there in the mutant. Similar to the WT an increase of ubiquitinated proteins can be observed at the centromeric and telomeric region. However the level is visibly reduced, compared to the *Smc1β* intensity profiles. Also in the mutant, TRF2 represents two signals at both ends of the sister chromatid with co-localizing ubiquitinated proteins. The results illustrate an overall altered pattern of ubiquitinated proteins in the mutant due to the replacement of one target for ubiquitination, suggesting Smc1β K361 to be ubiquitinated in wild type diakinesis oocytes and a role of it at the telomeric and centromeric region.

Ubiquitinated K361 on Smc1β is important to preserve telomere structure in Metaphase I

Within *Smc1β*$^{K361R/K361R}$ we observed chromosome structures which may appear comparable to structures seen in aged oocytes. Chromosomes of aged female oocytes show a characteristic loosened chromatin structure with an increased amount of distal CO (Liu and Keefe 2008). To study the importance of the post-translational modification on K361 for chromosomal integrity, metaphase I spreads were prepared and the DNA labelled.

Furthermore we co-stained for Crest, TRF2 and ubiquitinated proteins to gain a detailed view of their proteinaceous patterns.

In figure 12A a representative *Smc1β* oocyte in metaphase I is illustrated. The 20 chromosomes displayed visible chiasmata, a distinct pattern for the telomere protein TRF2 and for ubiquitinated proteins. For further analyzing the chromosomal structure, we focused on one particular chromosome structure that attract our attention (Fig. 12Ai). This chromosome structures were visible in *Smc1β* and *Smc1β*$^{K361R/K361R}$ but somehow these chromosomes displayed a more loosened configuration in the mutant.

In figure 12Ai a WT chromosome can be observed, which displayed the selected chromosome structure. Within the WT, the centromeric and telomeric region is more or less visible as a compact structure at both ends. Similar to our previous results, an increase of ubiquitinated proteins can be observed at the centromere and at the telomere.

Within the representative mutant oocyte, two different chromosomes were selected. Both show similar structural organization, one CO localized proximal and at the distal end of the chromosome cohesion seems to be lost. To further gain a detailed view of the distal chromosomal end, intensity profiles were established. A line was drawn across the distal end of the WT chromosome through the telomere end. The measured profile illustrates a continuous TRF2 signal at the telomere end co-localizing with the signaling for ubiquitinated proteins (Fig. 12B). Looking at the intensity profile of the first selected chromosome in the mutant cell (Fig. 12Aii), a gap between two TRF2 signals can be observed. Within the TRF2 intensities also ubiquitinated proteins are visible but are absent in the gap. The intensity profile of the second mutant chromosome (Fig. 12Aiii) represents an alternating but continuous TRF2 signal. However the profile for ubiquitinated proteins overlaps with the telomere profile only partially, displaying a gap in the middle of the TRF2 signal (Fig. 12D). These results indicate a co-localization of ubiquitinated proteins with the telomere protein TRF2 in diakinesis oocytes suggesting an important function of ubiquitinated proteins for preserving the telomere architecture which seems to be impaired when a target for ubiquitination is mutated in Smc1β.

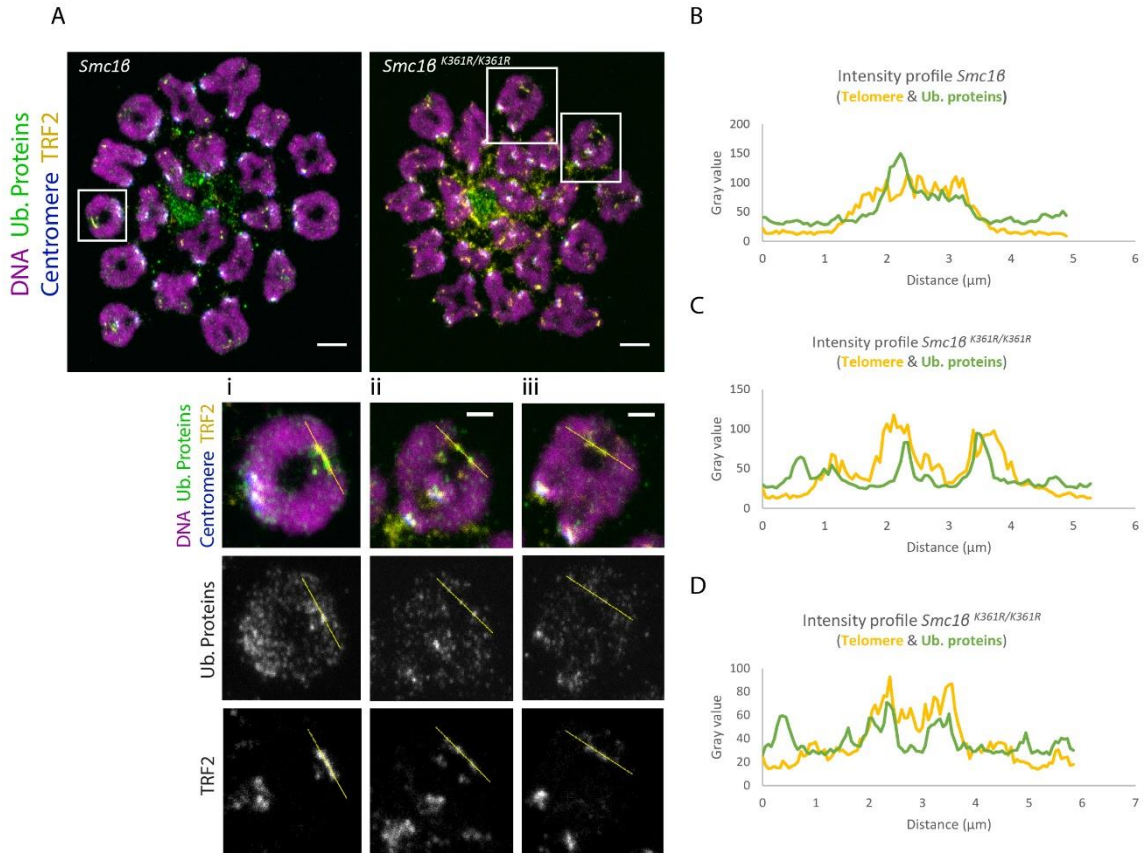

Figure 12. Aged phenotype visible in *Smc1β*$^{K361R/K361R}$ Metaphase I oocytes. (A) Two representative chromosome spreads of *Smc1β* and *Smc1β*$^{K361R/K361R}$ in Metaphase I, stained for DNA (Dapi), ubiquitinated proteins (FK2), Telomere (TRF2) and for centromeric region via Crest. Within the WT one chromosome was selected (white square) for detailed analyzation (i). An intensity profile was measured for the distal end of the chromosome (yellow line). Within the mutant two chromosomes were selected for intensity profile measurement (ii and iii). **(B)** The intensity profile of the WT distal chromosome end measured in (i). The measured telomere profile is represented by a yellow curve and the measured ub. proteins (green) overlap within the TRF2 intensity. **(C)** The intensity profile of the first selected mutant chromosome (ii). The TRF2 profile displays an interrupted curve with two intensities overlapping with ub. proteins. **(D)** The intensity profile of the second selected chromosome.

Ubiquitination of K361 on Smc1β is important for sister-kinetochore cohesion

During meiosis SMC1β display a distinctive pattern, starting to assemble along the chromatid with the onset of leptotene. Along the DNA SMC1β is stabilized until diplotene and with the onset of metaphase I SMC1β is removed from chromosome arms but remains at the centromeric region (Revenkova et al. 2001). Based on the specific localization of SMC1β

during meiotic progression and the fact that in *Smc1β*$^{-/-}$ the probability for aneuploidy is increased (Hodges et al. 2005) one can assume an essential role of SMC1β in sister chromatid cohesion.

To address whether the post-translational modification of SMC1β is important to fulfill its cohesive function, we analyzed oocytes in metaphase I. Previous results of *Smc1β*$^{-/-}$ diakinesis-metaphase I oocytes isolated from 2 months old mice revealed an increase of univalents when SMC1β is deficient (Hodges et al. 2005). We were not able to observe univalent chromosomes or chromosome fragments in 10 weeks old *Smc1β*$^{K361R/K361R}$ metaphase I oocytes. Nevertheless, we asked ourselves whether our mutant displays cohesion weakening at centromeres visible as a separation of the sister kinetochores in metaphase I. Therefore, metaphase I chromosomes were immunostained for chromatin (Dapi) and the centromeric region via Crest. In figure 13A a representative chromosome spread of a *Smc1β* oocyte in diakinesis is illustrated, containing chromosomes displaying visible chiasmata. To analyze weakened cohesion within *Smc1β*$^{K361R/K361R}$ oocytes, we compared the distance between sister kinetochores relative to the distances in our control strain. A *Smc1β*$^{K361R/K361R}$ chromosome spread of a diakinesis oocyte with chiasmata formation can be observed in fig. 13A. To measure the distance as accurate as possible, it was important to us gaining the highest resolution for microscopy imaging. Therefore cells were imaged with a laser scanning microscope containing Airyscan technology. Imaging of the centromeric region using airyscan mode resulted in a much higher resolution and sister kinetochores become visible in a resolved way. A representative pair of kinetochores can be observed in a magnified image for *Smc1β* and *Smc1β* $^{K361R/K361R}$ in figure 13A. For measuring the sister kinetochore distance, we used the program Imaris. This program recognizes the brightest point within one kinetochore and defines this as the center. The distance is then measured between the two centers of the kinetochore pair. If a pair of kinetochore is too close together, only one center could be determined resulting in an unresolved dataset. Within *Smc1β* oocytes, isolated from 10 weeks old females, the mean distance of sister kinetochores is 0.3576±0.007107µm. To avoid falsifying of measurements also the amount of unresolved pairs were included. In contrast, pairs of sister kinetochores measured in *Smc1β*$^{K361R/K361R}$ displayed a significant increase in median distance up to 0.424±0.005613µm.

Looking closer at the distribution of sister kinetochore distances, uncovers a visible shift of *Smc1β*$^{K361R/K361R}$ kinetochore distances towards a bigger distance (Fig 13C) compared to the WT. As expected, the WT cells contained more unresolved kinetochore pairs (~18%) due to the close association. Whereas in the mutant only 12% of the kinetochore pairs stayed unresolved. Looking closer at the distance distribution in *Smc1β* a hypothetical curve can be observed with the highest amount of kinetochore pairs displaying a distance 0.36-0.40µm. Within the mutant the highest point of the curve is shifted towards the distance 0.41-0.45µm, illustrating an increase of sister kinetochore distance in *Smc1β*$^{K361R/K361R}$. This indicates an overall increased kinetochore distance in *Smc1β*$^{K361R/K361R}$ oocytes suggesting a cohesive role of Smc1β K361 at the centromeric region.

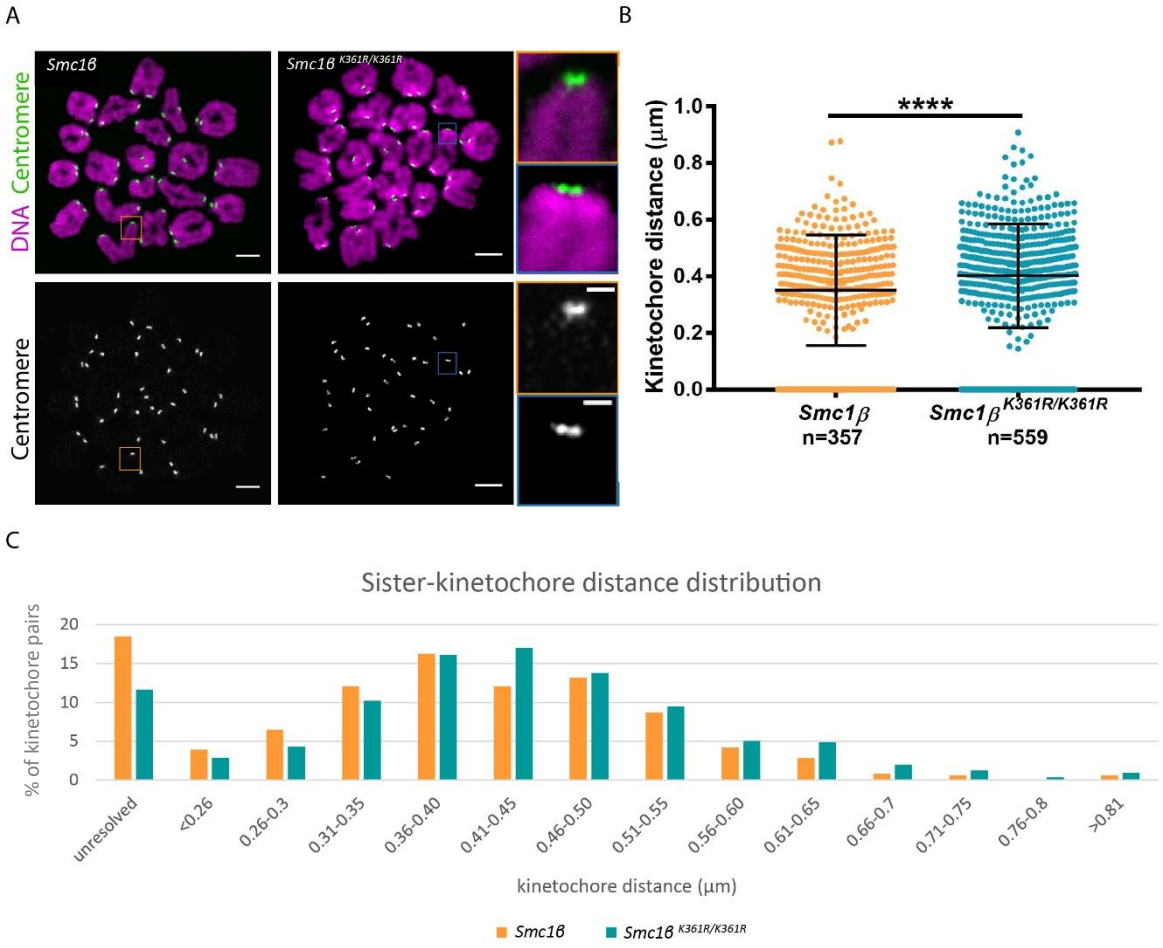

Figure 13. Smc1β K361 promotes sister kinetochore cohesion in Metaphase I oocytes. (A) Representative images of *Smc1β* and *Smc1β* $^{K361R/K361R}$ diakinesis oocytes isolated from 2 month old females. DNA was labelled by Dapi staining (magenta) and the centromeric region via Crest (green). Magnified images represent an exemplary pair of kinetochores on a WT (orange square) or mutant (blue square) chromosome. **(B)** Comparison

of measured sister kinetochore distances within *Smc1β* and *Smc1β* $^{K361R/K36!R}$. Distances between 357 WT and 559 mutant kinetochore pairs were measured by using Imaris software. Within the mutant the mean distance (0.4018 µm) is significantly increased by 0.05 µm compared to the WT (0.3507 µm); p-value <0.0001. **(C)** Calculated sister kinetochore distance distribution of the WT (orange) compared to the mutant (blue).

Age-related increasing sister kinetochore distance in *Smc1β* $^{R363Q/R363Q}$

The fact that our second mutant *Smc1β*$^{R363Q/R363Q}$ displayed, similar to our first mutant (*Smc1β*$^{K361R/K361R}$), recombination defects we asked whether we can also observe a difference between sister kinetochore distance.

First we examined the oocytes of 10 weeks old females and compared the distances between pairs of kinetochores. Again airyscan technology was used to image stained chromosome spreads for DNA (Dapi) and the centromere (Crest) in order to achieve highest resolution. Already during taking images we were able to observe a greater distance between *Smc1β*$^{R363Q/R363Q}$ sister kinetochores. A representative pair of mutant kinetochores can be seen as two resolved dots in a magnified image (Fig. 13A). In comparison one WT centromere is shown, displaying a tight association of the kinetochore pair.

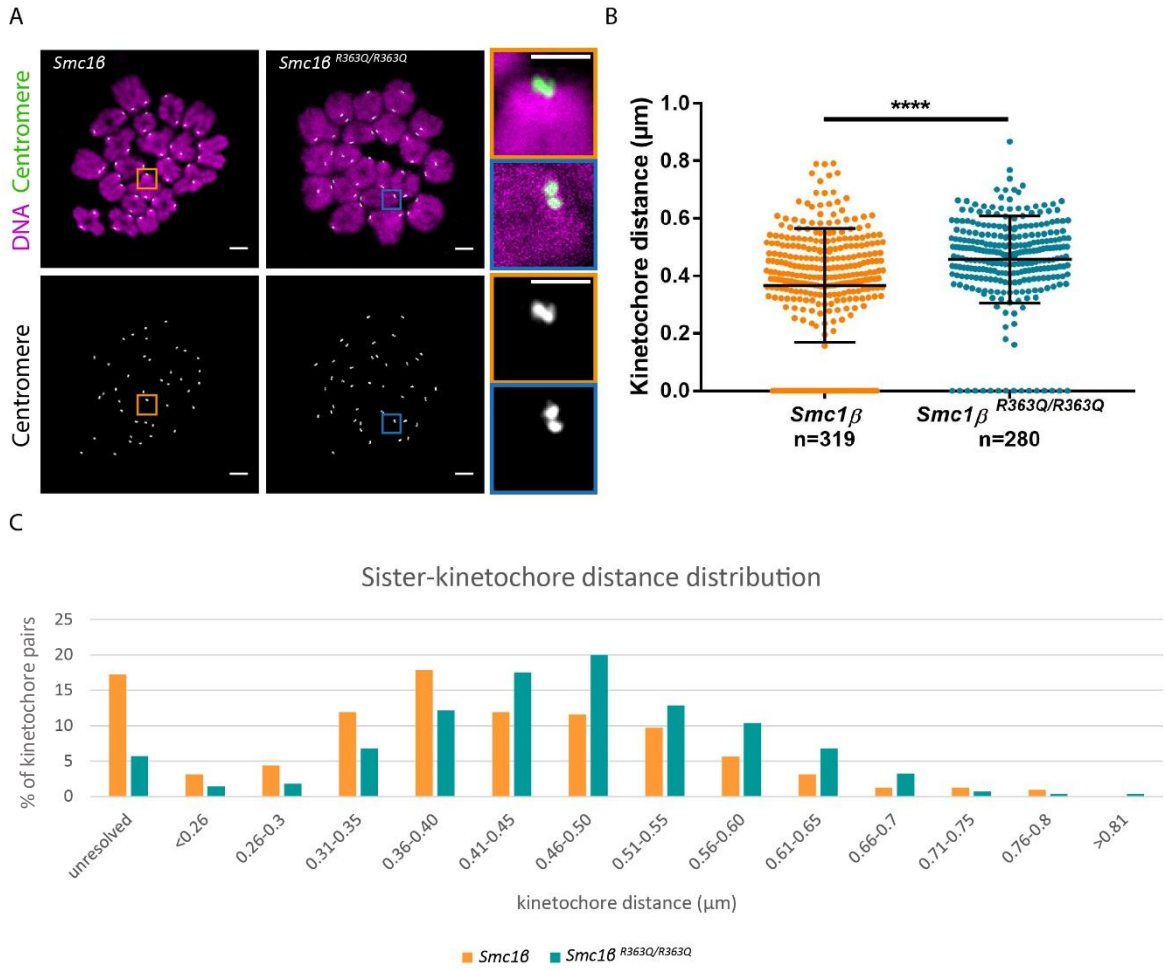

Figure 14. Smc1β R363 promotes sister kinetochore cohesion in 10 weeks old females Metaphase I oocytes. **(A)** Immunostaining of representative *Smc1β* and *Smc1β* $^{R363Q/R363Q}$ diakinesis oocytes isolated from 2 month old females. DNA was labelled by Dapi staining (magenta) and the centromeric region via Crest (green). Crest was imaged via airyscan and Dapi via confocal mode. Magnified images represent an exemplary pair of kinetochores on a WT (orange square) or mutant (blue square) chromosome. **(B)** Comparison of measured sister kinetochore distances within *Smc1β* and *Smc1β* $^{R363Q/R363Q}$. Distances between 319 WT and 280 mutant kinetochore pairs were measured by using Imaris software. Within the mutant the mean distance (0.457 µm) is significantly increased by 0.09 µm compared to the WT (0.3665 µm); p-value <0.0001. **(C)** Calculated sister kinetochore distance distribution of the WT (orange) compared to the mutant (blue). A shift towards bigger distances in the mutant can be observed.

From 319 *Smc1β* sister kinetochore pairs the distances were collected and compared to 280 measured *Smc1β*$^{R363Q/R363Q}$ kinetochore pairs (Fig. 14B). Within the control cells a mean sister kinetochore distance of 0.3665±0.01108µm was measured. In contrast, in the 10 weeks old mutant the sister kinetochore distance was significantly increased (0.457±0.00906µm) compared to the WT. This is also demonstrated in the detailed graph below representing the

sister kinetochore distance distribution (Fig. 14C). Around 17% of the WT kinetochore pairs remained unresolved whereas in the mutant 94 % of the kinetochore pairs were resolved and measured. Similar to the control used in the previous experiment, this control cells displayed a similar distance distribution, with the highest amount of pairs having a distance of 0.36-0.40µm. In contrast, 72.1% of the measured *Smc1β*$^{R363Q/R363Q}$ kinetochore pairs displayed a greater distance than 0.40µm. 17.5% of the measured mutant kinetochore pairs had a distance of 0.41-0.45µm and 20% a distance of 0.46-0.50µm.

A correlation between age-related loss of cohesion and SMC1β deficiency was already described for the full SMC1β knock-out. In SMC1β deficient female mice, an increase of unpaired univalents was reported to arise in an age dependent manner. Oocytes from six months old *Smc1β*$^{-/-}$ females contain only univalents or single chromatids, whereas in the WT all of the homologs form bivalent structures (Hodges et al. 2005). In our mutant female mice, aged six months, we were not able to observe any unpaired univalents or single chromatids in diakinesis oocytes. The same is true for oocytes isolated from our six month old control female (Fig. 15A). However within the WT cells the median sister kinetochore distance was increased (0.4545±0.009059µm) compared to the 10 weeks old females (0.3665±0.01108µm). In the six month old mutant mice the distance between sister kinetochores is further increased (0.5525±0.01159µm) compared to the 10 weeks old mutant females (0.457±0.00906µm). Furthermore we could observe a correlation between the increased distance in 10 weeks old mutant females and the increase of kinetochore distance in six month old WT females. Both displayed a similar median distance (~ 0.45 µm for both) and 17.85% of the measured WT kinetochore pairs were categorized with a distance between 0.46-0.5µm. Therefore we conclude that the 10 weeks old mutant displays a phenotype comparable to an aged WT female mice. The distance is also significantly greater in a mutant female (0.55µm) than in a WT female (0.45µm), when both are 6 month old. The distance distribution of 6 month old mutant females also showed a shift towards an increased kinetochore distance containing more than 40% with a greater distance than 0.46µm. Furthermore, more than 20% of the measured mutant kinetochore pairs displayed a greater distance than 0.66µm, whereas in the WT bigger distances than 0.65µm become rare. These results suggests a correlation of

increased age and separating sister kinetochores, indicating loss of centromeric cohesion which is even more pronounced by mutating one single amino residue of Smc1β.

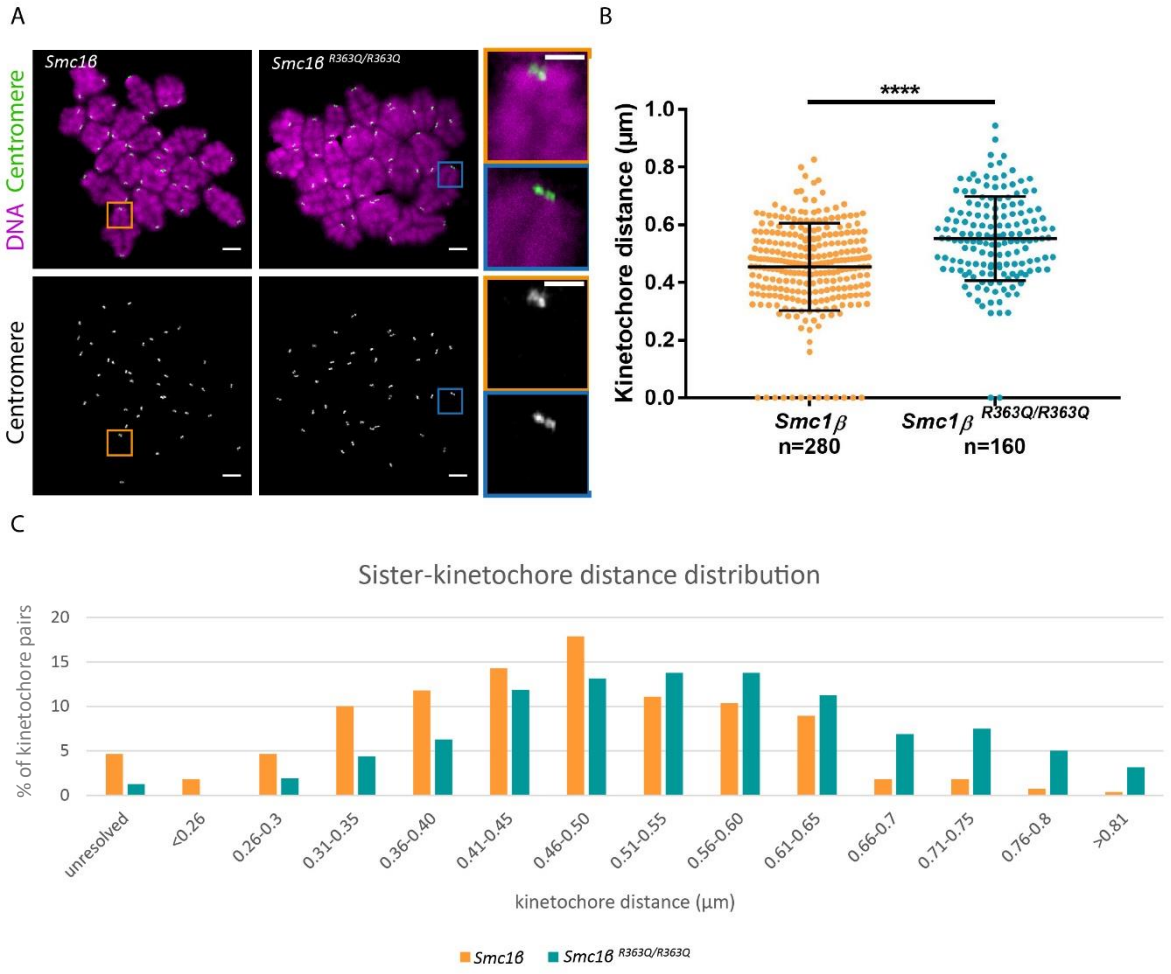

Figure 15. Smc1β R363 promotes sister kinetochore cohesion in 6-months old females Metaphase I oocytes. (A) Representative *Smc1β* and *Smc1β* $^{R363Q/R363Q}$ diakinesis oocytes isolated from 6 month old females, stained for DNA via Dapi and centromere by Crest. For imaging the centromeric region airyscan technology was used, whereas Dapi was imaged in confocal mode. Magnified images represent an exemplary pair of kinetochores on a WT (orange square) or mutant (blue square) chromosome. **(B)** Comparison of measured sister kinetochore distances within *Smc1β* and *Smc1β* $^{R363Q/R363Q}$. Distances between 280 WT and 160 mutant kinetochore pairs were measured by using Imaris software. Within the mutant the mean distance (0.5525 µm) is significantly increased by 0.098 µm compared to the WT (0.4545 µm); p-value <0.0001. **(C)** Calculated sister kinetochore distance distribution of the WT (orange) compared to the mutant (blue). A shift towards bigger distances in the mutant can be observed.

Discussion

The establishment and maintenance of sister chromatid cohesion facilitated by cohesin complexes is an essential requirement for proper chromosome segregation during meiosis. However little is known about the mechanism and regulation of the cohesin components in mammalian meiosis. More than a decade ago the specific isoform of cohesin component SMC1, named SMC1β, was identified but its role together with regulating proteins for stabilizing sister chromatid cohesion still needs to be elucidated. In spermatocytes SMC1β was shown to assemble with the onset of leptotene and remains on chromosome arms until metaphase I. The persistance at the centromeric region until anaphase II suggests an essential role of SMC1β as a regulator for centromeric sister chromatid cohesion during meiotic progression (Revenkova et al. 2001). Our results further extend the previous findings that SMC1β plays a role in centromeric cohesion (Biswas et al. 2013) and suggests it to be important for cross over maintenance. Here we provide an insight into an altered function of SMC1β due to the mutation of a single amino acid within the protein sequence. This suggests either a functional or structural regulation by the particular amino acid on Smc1β.

In order to study the outcome of mutating two selected amino residues, K361 and R363, on Smc1β we analyzed by immunofluorescence meiotic recombination, centromeric cohesion and telomere organization during meiotic progression in wild-type and mutant female oocytes.

A possible role of Smc1β K361 for preserving cross-over maintenance

We describe here a critical role of K361 on Smc1β for maintaining cross-over designated sites until they get resolved in diakinesis. Previous studies in SMC1β deficient mice revealed a correlation between the length of synaptonemal complex and frequency of recombination (Hodges et al. 2005). Here we show that mutating one lysine residue on Smc1β leads to a significant difference in the rate of exchange visible at the SC. Although $Smc1\beta^{K361R/K361R}$ pachytene cells display a reduced level of MLH1 foci (Fig. 3), we were not able to observe a shortening of the SC (data not shown).

The MutL protein 1 represents a regulator for cross-over resolution via the cross-over interfering pathway. It associates to sites of DSB and thereby reflects sites for recombination (reviewed by Baudat et al. 2013). Our data confirm this correlation by showing a similar distribution of cross-over, visible as chiasmata in metaphase I, and the corresponding cross-over in wild-type pachytene cells. Our experiment shows a reduced level of cross-over designated sites by 15% when K361 is mutated, however this is not arising in context with a shorter synaptonemal complex. It is not clear whether the reduced level of MLH1 foci is due to a deficient synaptonemal complex or a delayed progression of meiotic recombination. Given that oocytes, deficient for proper axial element formation develop further MLH1 foci assembly but display less recombination sites (~ 22 %) (De Boer et al. 2007) makes us confident to think about a possible relationship between the reduced rate of exchange and the formation of altered structures observed by SYCP3. We were not able to specifically characterize the defects found during formation of the synaptonemal complex in $Smc1\beta^{K361R/K361R}$ due to variability but the notable observation of only 19 completely synapsed axial elements (data not shown) in $Smc1\beta^{K361R/K361R}$ pachytene cells might either reflect a delay of homologous pairing or a defective SYCP3 assembly within those cases. The occurrence of altered axial element formations might correlate with the observation of incidental telomere defects. Although we were able to observe bouquet formation due to telomere association, telomere defects were detected either within the bouquet or in mid-pachytene. The occurrence of telomere bridges suggests a defective association of the telomere ends along the nuclear envelope which might affect an important support for homologous pairing. One could conceive a scenario where a deficient telomere association can lead to an altered homologous pairing, either by a delay or an impaired formation, and this further affects cross-over maturation.

Studies in SMC1β deficient female mice support the idea of a mechanistic role of cohesin in chiasma maintenance throughout meiotic progression (Hodges et al. 2005). Our data demonstrate a higher distorted cross-over distribution when K361 is mutated suggesting an important role of the lysine residue for cross over maintenance. Control cells displayed a reduced level of proximal localized cross-overs during the transition from pachytene to diakinesis with a correlative increase of central cross-overs. The shift towards the central

region of the chromosome axis could be due to a mechanism, responsible for inhibiting cross-over formation near the centromeric region, serving as a safeguard for proper chromosome segregation (Blitzblau et al. 2007). In the case of *Smc1β*$^{K361R/K361R}$ we observed a similar skewed distribution of proximal cross-overs towards the internal section of the chromosome. One could imagine the existence of an inhibitory mechanism to be responsible for this observation, nevertheless such a mechanism was so far only described in yeast (Rockmill et al. 2006). Unexpectedly, the number of multiple cross-overs was diminished by half in *Smc1β*$^{K361R/K361R}$ metaphase I oocytes. Concurrently the amount of central and distal localized cross-overs were increasing during the transition of cross-over designated sites to the formation of chiasmata. These results indicate an impairment for maintaining cross-overs due to the mutation of a single lysine residue on Smc1β, which further suggest an increased motility of designated cross-overs. An increased probability of distal chiasmata to slip off due to loss of cohesion was discussed in previous studies (Hodges et al. 2005). Our observations of an altered localization of the telomere protein TRF2, which is an important regulator for the telomere end organization might correlate with an increased chromosomal instability (Okamoto et al. 2013). In mammals TRF2 was shown to play an important role for the formation of the telomeric loop in order to support chromosome end protection (Stansel et al. 2001; Peuscher et al. 2012). Here we can only speculate cautiously whether an altered telomere structure or a loosened telomeric cohesion can provide cross-over shedding.

Detection of ubiquitinated proteins in Metaphase I oocytes

Given that the post-translational modification of proteins by ubiquitin represent an important way of protein regulation and due to the observation of Smc1β K361 to be ubiquitinated in spermatocytes, we analyzed the pattern of ubiquitinated proteins in metaphase I oocytes. Our results demonstrate a divergent level of ubiquitinated proteins visible on chromosomes when K361 is mutated. Intensity profiles of control oocytes revealed a distinct accumulation of ubiquitinated proteins at the centromeric and telomeric regions with an alternating distribution along the chromosome arm. In case of *Smc1β*$^{K361R/K361R}$ the level of ubiquitinated proteins was reduced along the chromosome arm, at the centromere and telomeres. Revenkova et al

postulated different SMC1β localizations in spermatocytes and female oocytes (Revenkova et al. 2001; Revenkova et al. 2010). In spermatocytes SMC1β is removed from chromosome arms in diplotene but remains at the centromeric region (Revenkova et al. 2001). A different pattern for SMC1β was described in mouse oocytes, with a distinct localization at the chromosome axis in metaphase I (Kouznetsova et al. 2005; Revenkova et al. 2010). Our results showing a reduced level of ubiquitinated proteins along the chromosome arm, when K361 is mutated, suggests a possible localization of SMC1β there in a wild-type metaphase I oocyte. However, from this data we cannot conclude that the overall reduced level of ubiquitinated proteins is due to loss of SMC1β or just a loss of an ubiquitin target.

By examining the distribution of ubiquitinated proteins at the chromosome ends, we were able to observe a visible coincidence with the telomere protein TRF2. This observation correlates with a reported regulation of telomere organization and maintenance by ubiquitination of telomere binding proteins (Broccoli et al. 1997; Peuscher et al. 2012). Besides the binding of the two shelterin components, TRF1 and TRF2, the telomere structure is further stabilized through the binding of RAP1, TIN2, TPP1 and POT1. Together these proteins represent the shelterin complex which provides several functions in telomere length organization, DNA damage response and telomere stability (reviewed by Peuscher et al. 2012). A signaling cascade via post-translational modification regulates the function of the shelterin components. For instance, one particular protein, named TPP1, is stabilized via ubiquitination at the telomere end, contributing to the telomere maintenance and stability (Peuscher et al. 2012). Our observation on *Smc1β*$^{K361R/K361R}$ metaphase I chromosomes, of less ubiquitinated proteins at the telocentric region could be a direct consequence of the mutated lysine residue of Smc1β. The fact that this particular lysine residue is not available anymore for ubiquitination might lead to an altered pattern of ubiquitinated proteins at the centromeric and telomeric region, where SMC1β is believed to localize in female oocytes (Kouznetsova et al. 2005). However, the reduced level of ubiquitinated proteins at the telocentric region overlaps more or less exactly with a reduced TRF2 signal. Here we should also not exclude our observation of a variable TRF2 staining within the control and the mutant strain. Nevertheless, our results prove a specific pattern of ubiquitinated proteins along the chromosome, which is altered due to the mutation of one single lysine residue on Smc1β.

Whether this is due to the loss of a target for ubiquitination on SMC1β or an altered regulation of Smc1β at the telomeric regions has to be considered but still needs to be proven.

Weakened centromere cohesion in replaced K361 Smc1β oocytes

Due to the observation in male meiocytes that SMC1β is loaded onto chromatin in early prophase, removed from chromosome arms in diplotene and remains only at the centromeric region implies a unique role of SMC1β at the centromere (Revenkova et al. 2001). Further studying the role of SMC1β in male meiosis by forcing pre-mature chromosome condensation of mid-pachytene cells revealed the function of SMC1β in cohesion maintenance along chromosome arm and centromere (Revenkova et al. 2004). Here we considered whether SMC1β is important for centromeric cohesion during female meiosis. To answer this question we measured sister kinetochore distance, which is thought to reflect cohesion holding centromeres together (Chiang et al. 2011). Our results demonstrate a cohesive role of SMC1β K361 at the centromere. We were able to observe a greater distance in case of the measured sister kinetochores in metaphase I oocytes of 10 weeks old $Smc1\beta^{K361R/K361R}$ females, compared to the age-matched control cells. This observation indicates a role of SMC1β K361 for centromeric cohesion, which is weakened when K361 is mutated.

Centromeric cohesion has to be established during meiotic progression and need to be maintained between sister chromatids until they segregate in anaphase II (Watanabe et al. 2012). To guarantee evenly distributed chromosomes after anaphase I, sister kinetochores need to be linked mono-oriented to the microtubules. In yeast premature loss of centromeric cohesion due to inactivation of Rec8 affects kinetochore geometry and thereby promotes bi-orientation at meiosis I which further result, in the worst case, in aneuploidy (Watanabe et al. 2012). In mammals REC8 provides sister chromatid cohesion until anaphase I and gets removed from chromosome arms due to separation of homolgous chromosomes (Tachibana-Konwalski et al. 2010). It remains at the centromere until anaphase II, together with SMC1β (Lee et al. 2003). Our results support the idea of an important role of SMC1β for preserving centromeric cohesion in female oocytes.

Altered MLH1 distribution due to mutating one single arginine residue of Smc1β

We next investigated the role of a second amino residue, R363, of Smc1β during mammalian meiosis by replacing R363 by either a glutamine (Q) or alanine (A). We described above the role of a lysine residue on Smc1β for preserving the integrity of correct cross over formation during meiotic progression. Similar to K361 this particular arginine was shown to be a target for post-translational modification. Szydlowska-Bylicka was able to isolate Smc1β from spermatocytes containing a methylated arginine residue (R363) (unpublished data, Anna Szydlowska-Bylicka). We first asked whether the frequency of MLH1 foci is altered when R363 is mutated. Although, both mutants (R363Q and R363A) displayed an obvious reduced number of MLH1 foci, we noticed a more pronounced phenotype in *Smc1β*$^{R363A/R363A}$. This observation indicates that the replacement of arginine 363 to an alanine is more efficient for preventing methylation. Same was also observed in yeast, where the function of a post-translational modification by methylation on histone H3 was studied. Changing the target amino acid into glutamine or alanine displayed different levels of phenotypical expression (Kirmizis et al. 2007). Rarely glutamine residues are found ubiquitinated in proteins (Tessarz et al. 2014), therefore we cannot exclude a complete prevention of methylation when arginine is replaced by glutamine. A stronger phenotype can be further explained by the loss of charge when arginine is replaced by alanine or it is a result of a conformational change due to the smaller structure of alanine (K. Tachibana-Konwalski, personal communication). The observation of a stronger phenotypic expression level (indicated by less MLH1 foci) in *Smc1β*$^{R363A/R363A}$ makes us confident to see R363 as a possible target for methylation and suggests that methylated R363 on Smc1β might be important for meiotic recombination in female meiocytes. Whether the reduced level of exchange correlate with a shorter synaptonemal complex or a defective axial element formation cannot be ruled out and has to be determined.

Age-dependent increase in sister kinetochore distance in *Smc1β*$^{R363Q/R363Q}$

In human an age-related increase of aneuploidy due to loss of sister chromatid cohesion was postulated. Although the aging effect is not that prominent in mice, a premature loss of cohesion at the centromeric region was shown to promote aneuploidy in aged female mice (Chiang et al. 2011). This observation is based on an increased distance of sister kinetochores indicating weakened centromeric cohesion (Chiang et al. 2011). Due to the specific localization of SMC1β at the centromeric region in male anaphase I meiocytes we asked whether SMC1β is important for centromeric cohesion in female oocytes and whether a correlation of age and an increased kinetochore distance can be observed. In SMC1β deficient mice an age-associated phenotype was already described based on an increase of univalents. Here we show kinetochore distance measurements in metaphase I oocytes in 10 weeks old compared to six months old females. The 10 weeks old control females displayed a mean kinetochore distance of 0.37 µm, which is slightly bigger than known from literature (Chiang et al. 2011). This might be due to an improved technique that was used here for imaging and measurement or due to different mouse strains. Interestingly, the inter kinetochore distance in 10 weeks old *Smc1β*$^{R363Q/R3663Q}$ metaphase I oocytes was obviously increased, displaying a mean kinetochore distance of 0.46 µm. This observation suggests an important role of R363 on Smc1β for holding sister kinetochores together and concurrently indicates a role of SMC1β at the centromere during female meiosis. Next we investigated the effect of replaced R363 in 6 months old female oocytes. Unexpectedly, we observed a similar increase in sister kinetochore distance in six month old control cells like it was measured for 10 weeks old mutant cells. Notably, the distance of sister kinetochores in six months old mutant cells was further increased when compared to the six month old wild type cell or to the 10 weeks old mutants. These results indicate an age-associate change in kinetochore distances, suggesting weakened centromeric cohesion with increasing age. The effect that 10 weeks old oocytes reflects a representative six month old wild type phenotype indicates a role of SMC1β for maintenance of centromeric cohesion in an age-dependent manner.

Conclusion

Here we provide an extended view of the importance of SMC1β for sister chromatid cohesion and its maintenance during female meiosis. The observation of a reduced number of MLH1 foci in all three mutants to more or less the same extend reflects either an important structural conformation which is altered when the amino acid chain is mutated at position 361 or 363 of Smc1β, or the amino residue itself provides an important function for recombination via a posttranslational modification by serving as a recruitment platform for interacting proteins (Fig. 16). Here we were not able to directly demonstrate that SMC1β is ubiquitinated at lysine 361 during female meiosis, however the observation of a reduced level of ubiquitinated proteins in *Smc1β*$^{K361R/K361R}$ metaphase I oocytes suggests a loss of targets for ubiquitination in the mutant. The increased separation of sister kinetochores in young and old mutants provide the view of SMC1β to be important for centromeric cohesion. Although we could not observe an increase of univalents or single chromatids with age, the 10 weeks old mutant display a representative sister kinetochore distance of a 6 month old wild type animal. This indicates a loss of function by SMC1β at the centromeric region increasing with age. Since the mutants do not display such a prominent phenotype than *Smc1β*$^{-/-}$ we can exclude that the selected amino residues are an essential requirement for binding of SMC1β to the chromatin structure. However the impaired maintenance of cross-over events suggests a role of the amino residues of Smc1β to maintain chromosome cohesion. We propose that this is due to loss of a target for a post-translational modification, which might lead to loss of a binding partner (Fig. 16).

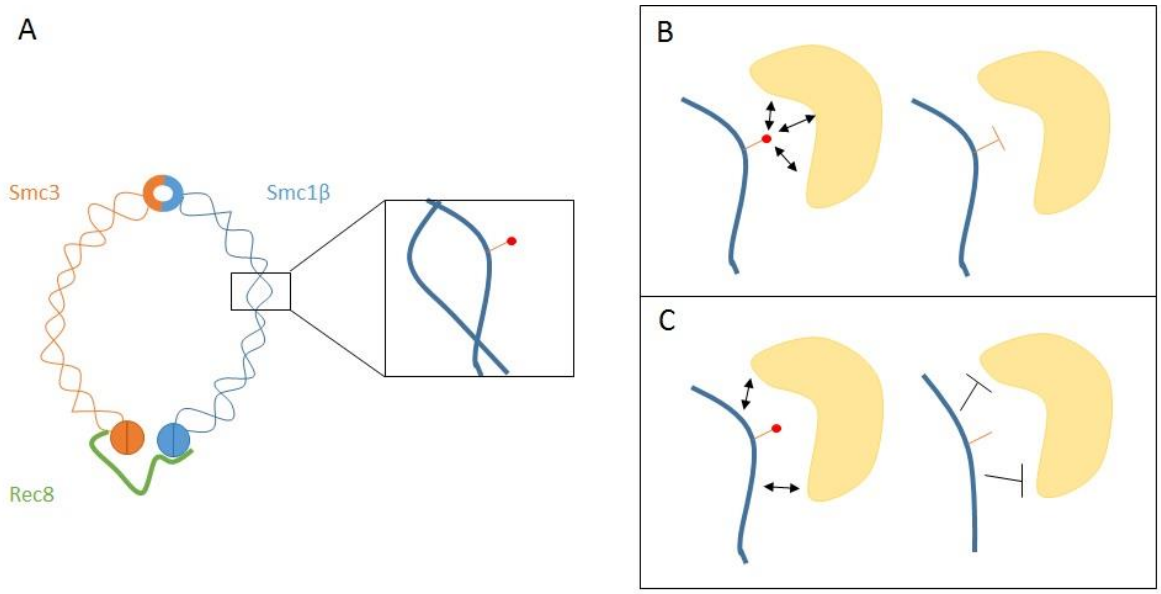

Figure 16. Model of post-translational modified cohesin complex as a requirement for protein binding. (A) The cohesin complex Smc3/Smc1β/Rec8 containing post-translational modified amino residue on Smc1β (magnified structure). **(B)** PTM is required for protein binding (yellow). **(C)** PTM causes conformational change required for protein binding.

References

Adelfalk, C., Janschek, J., Revenkova, E., Blei, C., Liebe, B., Göb, E., Alsheimer, M., Benavente, R., De Boer, E., Novak, I., Höög, C., Scherthan, H., Jessberger, R. (2009). Cohesin SMC1β protects telomeres in meiocytes. *Journal of Cell Biology*, *187*(2), 185–199.

Agostinho, A., Manneberg, O., Schendel, R. Van, Hernández-hernández, A., Kouznetsova, A., Blom, H., Brismar, H., Höög, C. (2016). High density of REC 8 constrains sister chromatid axes and prevents illegitimate synaptonemal complex formation, *17*(6), 1–13.

Alberts B., Bray D., Lewis J., Raff M., Roberts K., Watson J.D., Orme N., Hesketh-Moore K. (2005). *Lehrbuch der Molekularen Zellbiologie* (3rd ed.). WILEY-VCH Verlag GmbH & Co. KGaA. ISBN- 978-3-526-31160-6

Annunziato, A. (2008). DNA Packaging: Nucleosomes and Chromatin. *Nature Education*, *1*(1), 26.

Baudat, F., Imai, Y., & de Massy, B. (2013). Meiotic recombination in mammals: localization and regulation. *Nature Reviews. Genetics*, *14*(11), 794–806.

Bayliss, R., Littlewood, T., & Stewart, M. (2000). Structural basis for the interaction between FxFG nucleoporin repeats and importin-beta in nuclear trafficking. *Cell*, *102*(1), 99–108.

Bedford, M. T., & Clarke, S. G. (2009). Protein Arginine Methylation in Mammals: Who, What, and Why. *Molecular Cell*, *33*(1), 1–13.

Ben-shahar, T. R., Heeger, S., Lehane, C., East, P., Flynn, H., Skehel, M., & Uhlmann, F. (2008). Eco1-Dependent Cohesin Sister Chromatid Cohesion. *Science*, *321*(July), 563–566.

Biggar, K. K., & Li, S. S.-C. (2014). Non-histone protein methylation as a regulator of cellular signalling and function. *Nature Reviews. Molecular Cell Biology*, *16*(1), 5–17.

Bilaud, T., Brun, C., Ancelin, K., Koering, C. E., Laroche, T., & Gilson, E. (1997). Telomeric localization of TRF2, a novel human telobox protein. *Nature Genetics*, *17*(2), 236–9.

Bishop, D. K., & Zickler, D. (2004). Early decision: Meiotic crossover interference prior to stable strand exchange and synapsis. *Cell*, *117*(1), 9–15.

Bisig, C. G., Guiraldelli, M. F., Kouznetsova, A., Scherthan, H., Höög, C., Dawson, D. S., & Pezza, R. J. (2012). Synaptonemal complex components persist at centromeres and are required for homologous centromere pairing in mouse spermatocytes. *PLoS Genetics*, *8*(6).

Biswas, U., Wetzker, C., Lange, J., Christodoulou, E. G., Seifert, M., Beyer, A., & Jessberger, R. (2013). Meiotic Cohesin SMC1β Provides Prophase I Centromeric Cohesion and Is Required for Multiple Synapsis-Associated Functions. *PLoS Genetics*, *9*(12).

Blitzblau, H. G., Bell, G. W., Rodriguez, J., Bell, S. P., & Hochwagen, A. (2007). Mapping of Meiotic Single-Stranded DNA Reveals Double-Strand-Break Hotspots near Centromeres and Telomeres. *Current Biology*, *17*(23), 2003–2012.

Bohacek, J., & Mansuy, I. M. (2015). Molecular insights into transgenerational non-genetic inheritance of acquired behaviours. *Nature Reviews Genetics*, *16*(11), 641–652.

Brar, G. A., Kiburz, B. M., Zhang, Y., Kim, J., White, F., & Amon, A. (2006). Rec8 phosphorylation and recombination promote the step-wise loss of cohesins in meiosis, *441*(May), 10–14.

Broccoli, D., Smogorzewska, A., Chong, L., & de Lange, T. (1997). Human telomeres contain two distinct Myb-related proteins, TRF1 and TRF2. *Nature Genetics*, *17*(2), 231–5.

Burkhardt S., Borsos M., Szydlowska A., Godwin J., Williams S.A., Cohen P.E., Hirota T., Saitou M., Tachibana-Konwalski K. (2016). Chromosome Cohesion Established by Rec8- Cohesin in Fetal Oocytes Is Maintained without Detectable Turnover in Oocytes Arrested for Months in Mice. *Current Biology*, *26*(5), 678–85.

Chiang, T., Duncan, F. E., Schindler, K., Schultz, R. M., & Michael, A. (2011). Evidence that weakened centromere cohesion is a leading cause of age-related aneu-ploidy in oocytes, *20*(17), 1522–1528.

Chikashige, Y., Haraguchi, T., & Hiraoka, Y. (2007). Another way to move chromosomes. *Chromosoma*, *116*(6), 497–505.

Cong, L., Ran, F. A., Cox, D., Lin, S., Barretto, R., Hsu, P. D., Wu, X., Jiang, W., Marraffini, L. A. (2013). Multiplex Genome Engineering Using CRISPR/Cas Systems. *Science*, *339*(6121), 819–823.

De Boer, E., Dietrich, A. J. J., Höög, C., Stam, P., & Heyting, C. (2007). Meiotic interference among MLH1 foci requires neither an intact axial element structure nor full synapsis. *Journal of Cell Science*, *120*, 731–6.

De La Fuente, R., Parra, M. T., Viera, A., Calvente, A., Gómez, R., Suja, J. Á., Rufas, J. S. Page, J. (2007). Meiotic pairing and segregation of achiasmate sex chromosomes in eutherian mammals: The role of SYCP3 protein. *PLoS Genetics*, *3*(11), 2122–2134.

Ding, D. Q., Matsuda, A., Okamasa, K., Nagahama, Y., Haraguchi, T., & Hiraoka, Y. (2016). Meiotic cohesin-based chromosome structure is essential for homologous chromosome pairing in Schizosaccharomyces pombe. *Chromosoma*, *125*(2), 205–214.

Dorsett, D., Eissenberg, J. C., Misulovin, Z., Martens, A., Redding, B., & McKim, K. (2005). Effects of sister chromatid cohesion proteins on cut gene expression during wing development in Drosophila. *Development (Cambridge, England)*, *132*(21), 4743–53.

Eijpe, M., Heyting, C., Gross, B., & Jessberger, R. (2000). Association of mammalian SMC1 and SMC3 proteins with meiotic chromosomes and synaptonemal complexes, *682*, 673–682.

Eijpe, M., Offenberg, H., Jessberger, R., Revenkova, E., & Heyting, C. (2003). Meiotic cohesin REC8 marks the axial elements of rat synaptonemal complexes before cohesins SMC1β and SMC3. *Journal of Cell Biology*, *160*(5), 657–670.

Fraune, J., Schramm, S., Alsheimer, M., & Benavente, R. (2012). The mammalian synaptonemal complex: Protein components, assembly and role in meiotic recombination. *Experimental Cell Research*, *318*(12), 1340–1346.

Fukuda, T., Daniel, K., Wojtasz, L., Toth, A., & Höög, C. (2010). A novel mammalian HORMA domain-containing protein, HORMAD1, preferentially associates with unsynapsed meiotic chromosomes. *Experimental Cell Research*, *316*(2), 158–171.

Gandhi, R., Gillespie, P. J., & Hirano, T. (2006). Human Wapl Is a Cohesin-Binding Protein that Promotes Sister-Chromatid Resolution in Mitotic Prophase. *Current Biology*, *16*(24), 2406–2417.

Garcia-Cruz, R., Brieño, M. A., Roig, I., Grossmann, M., Velilla, E., Pujol, A., Cabero, L., Pessarrodona, A., Barbero, J.L., Garcia Caldés, M. (2010). Dynamics of cohesin proteins REC8, STAG3, SMC1β and SMC3 are consistent with a role in sister chromatid cohesion during meiosis in human oocytes. *Human Reproduction*, *25*(9), 2316–2327.

Gilbert SF. (2000). *Developmental Biology* (6th ed.). Sunderland (MA): Sinauer Associates. ISBN- 0-87893-243-7

Glozak, M. A., Sengupta, N., Zhang, X., & Seto, E. (2005). Acetylation and deacetylation of non-histone proteins. *Gene*, *363*(1-2), 15–23.

Graves J. D. and Edwin G. Krebs. (1999). Protein Phosphorylation and Signal Transduction. *Pharmacology & Therapeutics*, *82*(2-3), 111–121.

Grillari J., Grillari-Voglauer R., and J.-D. P. (2010). Post-Translational Modification of Cellular Proteins by Ubiquitin and Ubiquitin-Like Molecules: Role in Cellular Senescence and Ageing. *Landes Bioscience and Springer Science+Business Media*, *694*, 172–96.

Gutiérrez-Caballero, C., Herrán, Y., Sánchez-Martín, M., Suja, J. Á., Barbero, J. L., Llano, E., & Pendás, A. M. (2011). Identification and molecular characterization of the mammalian α-kleisin RAD21L. *Cell Cycle*, *10*(9), 1477–1487.

Haas A. L., Siepmann. T. J. (1997). Pathways of ubiquitin conjugation. *FASEB J*, *11*(14), 1257–68.

Handel, M. A., & Schimenti, J. C. (2010). Genetics of mammalian meiosis: regulation, dynamics and impact on fertility. *Nature Reviews. Genetics*, *11*(2), 124–136.

Harper, L., Golubovskaya, I., & Cande, W. Z. (2004). A bouquet of chromosomes. *Journal of Cell Science*, *117*(Pt 18), 4025–4032.

Hartman, T., Stead, K., Koshland, D., & Guacci, V. (2000). Pds5p is an essential chromosomal protein required for both sister chromatid cohesion and condensation in Saccharomyces cerevisiae. *Journal of Cell Biology*, *151*(3), 613–626.

Hassold, T., & Hunt, P. (2001). To err (meiotically) is human: the genesis of human aneuploidy. *Nature Reviews. Genetics*, *2*(4), 280–291.

Hernández-Hernández, A., Masich, S., Fukuda, T., Kouznetsova, A., Sandin, S., Daneholt, B., & Höög, C. (2016). The central element of the synaptonemal complex in mice is organized as a bilayered junction structure. *Journal of Cell Science*, (April), 2239–2249.

Herrán, Y., Gutiérrez-Caballero, C., Sánchez-Martín, M., Hernández, T., Viera, A., Barbero, J. L., De Álava, E., de Rooij, D. G., Suja, J. A., Llano, E., Pendás, A. M. (2011). The cohesin subunit RAD21L functions in meiotic synapsis and exhibits sexual dimorphism in fertility. *The EMBO Journal*, *30*(15), 3091–3105.

Hodges, C. a, Revenkova, E., Jessberger, R., Hassold, T. J., & Hunt, P. a. (2005). SMC1beta-deficient female mice provide evidence that cohesins are a missing link in age-related nondisjunction. *Nature Genetics*, *37*(12), 1351–1355.

Ishiguro, K. I., Kim, J., Shibuya, H., Hernández-Hernández, A., Suzuki, A., Fukagawa, T., Shioi, G., Kiyonari, H., Li, X., Schimenti, J., Höög, C., Watanabe, Y. (2014). Meiosis-specific cohesin mediates homolog recognition in mouse spermatocytes. *Genes and Development*, *28*(6), 594–607.

Ishiguro, K., Kim, J., Fujiyama-Nakamura, S., Kato, S., & Watanabe, Y. (2011). A new meiosis-specific cohesin complex implicated in the cohesin code for homologous pairing. *EMBO Reports*, *12*(3), 267–275.

Ishiguro, K., & Watanabe, Y. (2007). Chromosome cohesion in mitosis and meiosis. *J Cell Sci.*, *120*(Pt 3), 367–9.

Ivanov, D., Schleiffer, A., Eisenhaber, F., Mechtler, K., Haering, C. H., & Nasmyth, K. (2002). Eco1 is a novel acetyltransferase that can acetylate proteins involved in cohesion. *Current Biology*, *12*(4), 323–328.

Jessberger, R. (2002). The many functions of SMC proteins in chromosome dynamics. *Nat Rev Mol Cell Biol*, *3*(10), 767–778.

Kim, H. S., Kim, S. H., Park, H. Y., Lee, J., Yoon, J. H., Choi, S., Ryu, S. H., Lee, H., Cho, H. S., Lee, C. W. (2013). Functional interplay between Aurora B kinase and Ssu72 phosphatase regulates sister chromatid cohesion. *Nat Commun*, *4*, 2631.

Kirmizis, A., Santos-Rosa, H., Penkett, C. J., Singer, M. A., Vermeulen, M., Mann, M., Bähler, J., Green, R. D., Kouzarides, T. (2007). Arginine methylation at histone H3R2 controls deposition of H3K4 trimethylation. *Nature*, *449*(7164), 928–932.

Kitajima, T. S., Sakuno, T., Ishiguro, K., Iemura, S., Natsume, T., Kawashima, S. a, & Watanabe, Y. (2006). Shugoshin collaborates with protein phosphatase 2A to protect cohesin. *Nature*, *441*(7089), 46–52.

Klein, F., Mahr, P., Galova, M., Buonomo, S. B. C., Michaelis, C., Nairz, K., & Nasmyth, K. (1999). A central role for cohesins in sister chromatid cohesion, formation of axial elements, and recombination during yeast meiosis. *Cell*, *98*(1), 91–103.

Kouznetsova, A., Benavente, R., Pastink, A., & Höög, C. (2011). Meiosis in Mice without a Synaptonemal Complex. *PLoS One*, *6*(12), e28255.

Kouznetsova, A., Novak, I., Jessberger, R., & Hoog, C. (2005). SYCP2 and SYCP3 are required for cohesin core integrity at diplotene but not for centromere cohesion at the first meiotic division. *J Cell Sci*, *118*(Pt 10), 2271–2278.

Kueng, S., Hegemann, B., Peters, B. H., Lipp, J. J., Schleiffer, A., Mechtler, K., & Peters, J. M. (2006). Wapl Controls the Dynamic Association of Cohesin with Chromatin. *Cell*, *127*(5), 955–967.

Ladurner, R., Bhaskara, V., Huis In 'T Veld, P. J., Davidson, I. F., Kreidl, E., Petzold, G., & Peters, J. M. (2014). Cohesin's ATPase activity couples cohesin loading onto DNA with Smc3 acetylation. *Current Biology*, *24*(19), 2228–2237.

Ladurner, R., Kreidl, E., Ivanov, M. P., Ekker, H., Idarraga-Amado, M. H., Busslinger, G. A., Wutz, G., Cisneros, D. A.,Peters, J. (2016). Sororin actively maintains sister chromatid cohesion. *The EMBO Journal*, *35*(6), 635–653.

Lee, J., Iwai, T., Yokota, T., & Yamashita, M. (2003). Temporally and spatially selective loss of Rec8 protein from meiotic chromosomes during mammalian meiosis. *J Cell Sci*, *116*(Pt 13), 2781–2790.

Lee, J., & Hirano, T. (2011). RAD21L, a novel cohesin subunit implicated in linking homologous chromosomes in mammalian meiosis. *Journal of Cell Biology*, *192*(2), 263–276.

Liu, L., & Keefe, D. L. (2008). Defective cohesin is associated with age-dependent misaligned chromosomes in oocytes. *Reproductive BioMedicine Online*, *16*(1), 103–112.

Llano, E., Herrán, Y., García-Tuñón, I., Gutiérrez-Caballero, C., de Álava, E., Barbero, J. L., Schimenti, J., de Rooij, D. G., Sánchez-Martín, M., Pendás, A. M. (2012). Meiotic cohesin complexes are essential for the formation of the axial element in mice. *Journal of Cell Biology*, *197*(7), 877–885.

Longo, F. J. (1973). Fertilization: A comparative ultratructural review. *Biol. Reprod.*, *9*, 149–215.

Losada, A., Yokochi, T., Kobayashi, R., & Hirano, T. (2000). Identification and characterization of SA/Scc3p subunits in the Xenopus and human cohesin complexes. *Journal of Cell Biology*, *150*(3), 405–416.

Losada, A., Yokochi, T., & Hirano, T. (2005). Functional contribution of Pds5 to cohesin-mediated cohesion in human cells and Xenopus egg extracts. *Journal of Cell Science*, *118*(Pt 10), 2133–2141.

Manchado, E., Eguren, M., & Malumbres, M. (2010). The anaphase-promoting complex/cyclosome (APC/C): cell-cycle-dependent and -independent functions. *Biochemical Society Transactions*, *38*(1), 65–71.

Mannini, L., Cucco, F., Quarantotti, V., Amato, C., Tinti, M., Tana, L., Frattini, A., Delia, D., Krantz, I. D., Jessberger, R., Musio, A. (2015). SMC1B is present in mammalian somatic cells and interacts with mitotic cohesin proteins. *Scientific Reports*, *5*, 18472.

Marston, A. L., & Amon, A. (2004). Meiosis: cell-cycle controls shuffle and deal. *Nature Reviews. Molecular Cell Biology*, *5*(12), 983–997.

Martinez-Perez, E., & Colaiácovo, M. P. (2009). Distribution of meiotic recombination events: talking to your neighbors. *Current Opinion in Genetics and Development*, *19*(2), 105–112.

May, M. J., & Ghosh, S. (1998). Signal transduction through NF-κB. *Immunology Today*, *19*(2), 80–88.

McLaughlin, E. A., & McIver, S. C. (2009). Awakening the oocyte: Controlling primordial follicle development. *Reproduction*, *137*(1), 1–11.

Molnar, M., Bahler, J., Sipiczki, M., & Kohli, J. (1995). The rec8 gene of Schizosaccharomyces pombe is involved in linear element formation, chromosome pairing and sister-chromatid cohesion during meiosis. *Genetics*, *141*(1), 61–73.

Müller-Esterl, W., Anderka, O., Brandt, U., & Kerscher, S. (2011). *Biochemie Eine Einführung für Mediziner und Naturwissenschaftler* (2. ed.). Spektrum Akademischer Verlag Heidelberg. ISBN- 978-3-8274-2003-9

Nagy A, Gerstenstein M, Vintersten K, B. R. (2003). *Manipulationg the Mouse Embryo* (3rd ed.). Cold Spring Harbor: Cold Spring Harbor Laboratory Press.

Nasmyth, K., & Haering, C. H. (2009). Cohesin: Its Roles and Mechanisms. *Annual Review of Genetics*, *43*, 525–558.

Neuwald, A. F. (2000). HEAT Repeats Associated with Condensins, Cohesins, and Other Complexes Involved in Chromosome-Related Functions. *Genome Research*, *10*(10), 1445–1452.

Nishiyama, T., Ladurner, R., Schmitz, J., Kreidl, E., Schleiffer, A., Bhaskara, V., Bando, M., Shirahige, K., Hyman, A. A., Mechtler, K., Peters, J. M. (2010). Sororin mediates sister chromatid cohesion by antagonizing Wapl. *Cell*, *143*(5), 737–749.

Nishiyama, T., Sykora, M. M., Mechtler, K., & Peters, J. (2013). Aurora B and Cdk1 mediate Wapl activation and release of acetylated cohesin from chromosomes by phosphorylating Sororin. *PNAS*, *110*(33), 13404–13409.

Oikawa, K., Ohbayashi, T., Kiyono, T., Nishi, H., Isaka, K., Umezawa, A., Kuroda, M., Mukai, K. (2004). Expression of a Novel Human Gene, Human Wings Apart-Like (hWAPL), Is Associated with Cervical Carcinogenesis and Tumor Progression, *Cancer Res. 64*(10), 3545–3549.

Okamoto, K., Bartocci, C., Ouzounov, I., K.Diedrich, J., Ill, J. R. Y., & Denchi, E. L. (2013). A two-step mechanism for TRF2-mediated chromosome end protection. *Nature*, *494*(7438), 502–505.

Ono, T., Losada, A., Hirano, M., Myers, M. P., Neuwald, A. F., & Hirano, T. (2003). Differential contributions of condensin I and condensin II to mitotic chromosome architecture in vertebrate cells. *Cell*, *115*(1), 109–121.

Parisi, S., McKay, M. J., Molnar, M., Thompson, M. a, van der Spek, P. J., van Drunen-Schoenmaker, E., Kanaar, R., Lehmann, E., Hoeijmakers, J. H., Kohli, J. (1999). Rec8p, a meiotic recombination and sister chromatid cohesion phosphoprotein of the Rad21p family conserved from fission yeast to humans. *Molecular and Cellular Biology*, *19*(5), 3515–3528.

Pasierbek, P., Jantsch, M., Melcher, M., Schleiffer, A., Schweizer, D., & Loidl, J. (2001). A Caenorhabditis elegans cohesion protein with functions in meiotic chromosome pairing and disjunction. *Genes & Development*, *15*(11), 1349–1360.

Parra, M. T., Viera, A., Gomez, R., Page, J., Benavente, R., Santos, J. L., Rufas, J. S., Suja, J. A. (2004). Involvement of the cohesin Rad21 and SCP3 in monopolar attachment of sister kinetochores during mouse meiosis I. *J Cell Sci*, *117*(Pt 7), 1221–1234.

Paudyal, A., Damrau, C., Patterson, V. L., Ermakov, A., Formstone, C., Lalanne, Z., Wells, S., Lu, X., Norris, D. P., Dean, C. H., Henderson, D. J., Murdoch, J. N. (2010). The novel mouse mutant, chuzhoi, has disruption of Ptk7 protein and exhibits defects in neural tube, heart and lung development and abnormal planar cell polarity in the ear. *BMC Developmental Biology*, *10*, 87.

Peuscher, M. H., & Jacobs, J. J. L. (2012). Posttranslational control of telomere maintenance and the telomere damage response. *Cell Cycle*, *11*(8), 1524–1534.

Pezzi, N., Prieto, I., Kremer, L., Pérez Jurado, L. A., Valero, C., Del Mazo, J., Martínez-a, C., Barbero, J. L. (2000). STAG3, a novel gene encoding a protein involved in meiotic chromosome pairing and location of STAG3-related genes flanking the Williams-Beuren syndrome deletion. *The FASEB Journal*, *14*(3), 581–592.

Prabakaran, S., Lippens, G., Steen, H., & Gunawardena, J. (2012). Post-translational modification: Nature's escape from genetic imprisonment and the basis for dynamic information encoding. *Wiley Interdisciplinary Reviews: Systems Biology and Medicine*, *4*(6), 565–583.

Prieto, I., Suja, J. a, Pezzi, N., Kremer, L., Martínez-A, C., Rufas, J. S., & Barbero, J. L. (2001). Mammalian STAG3 is a cohesin specific to sister chromatid arms in meiosis I. *Nature Cell Biology*, *3*(8), 761–766.

Rankin, S., Ayad, N. G., & Kirschner, M. W. (2005). Sororin, a substrate of the anaphase- promoting complex, is required for sister chromatid cohesion in vertebrates. *Molecular Cell*, *18*(2), 185–200.

Revenkova, E., Eijpe, M., Heyting, C., Gross, B., & Jessberger, R. (2001). Novel meiosis-specific isoform of mammalian SMC1. *Molecular and Cellular Biology*, *21*(20), 6984–6998. http://doi.org/10.1128/MCB.21.20.6984-6998.2001

Revenkova, E., Eijpe, M., Heyting, C., Hodges, C. A., Hunt, P. A., Liebe, B., Scherthan, H., Jessberger, R. (2004). Cohesin SMC1 beta is required for meiotic chromosome dynamics, sister chromatid cohesion and DNA recombination. *Nat Cell Biol*, *6*(6), 555–562.

Revenkova, E., Adelfalk, C., & Jessberger, R. (2010). Cohesin in Oocytes-Tough enough for Mammalian Meiosis? *Genes*, *1*(3), 495–504.

Riedel, C. G., Katis, V. L., Katou, Y., Mori, S., Itoh, T., & Helmhart, W. (2006). Protein phosphatase 2A protects centromeric sister chromatid cohesion during meiosis I. *Nature*, *441*(7089), 53-61.

Robert, T., Vrielynck, N., Mézard, C., de Massy, B., & Grelon, M. (2016). A new light on the meiotic DSB catalytic complex. *Seminars in Cell & Developmental Biology*, *54*, 165–176.

Rockmill, B., Voelkel-Meiman, K., & Roeder, G. S. (2006). Centromere-proximal crossovers are associated with precocious separation of sister chromatids during meiosis in Saccharomyces cerevisiae. *Genetics*, *174*(4), 1745–1754.

Roeder, G. S., & Bailis, J. M. (2000). The pachytene checkpoint. *Trends in Genetics*, *16*(9), 395–403.

Roje, S. (2006). S-Adenosyl-l-methionine: Beyond the universal methyl group donor. *Phytochemistry*, *67*(15), 1686–1698.

Schalk, J. A. C., Dietrich, A. J. J., Vink, A. C. G., Offenberg, H. H., Van Aalderen, M., & Heyting, C. (1998). Localization of SCP2 and SCP3 protein molecules within synaptonemal complexes of the rat. *Chromosoma*, *107*(8), 540–548.

Scherthan, H. (2007). Telomere attachment and clustering during meiosis. *Cellular and Molecular Life Sciences*, *64*(2), 117–124.

Scherthan, H., Jerratsch, M., Li, B., Smith, S., Hultén, M., Lock, T., & de Lange, T. (2000). Mammalian meiotic telomeres: protein composition and redistribution in relation to nuclear pores. *Molecular Biology of the Cell*, *11*(12), 4189–4203.

Schmitt, J., Benavente, R., Hodzic, D., Höög, C., Stewart, C. L., & Alsheimer, M. (2007). Transmembrane protein Sun2 is involved in tethering mammalian meiotic telomeres to the nuclear envelope. *Proceedings of the National Academy of Sciences of the United States of America*, *104*(18), 7426–31.

Schmitz, J., Watrin, E., Lénárt, P., Mechtler, K., & Peters, J. M. (2007). Sororin Is Required for Stable Binding of Cohesin to Chromatin and for Sister Chromatid Cohesion in Interphase. *Current Biology*, *17*(7), 630–636.

Schwertman, P., Bekker-Jensen, S., & Mailand, N. (2016). Regulation of DNA double-strand break repair by ubiquitin and ubiquitin-like modifiers. *Nature Reviews Molecular Cell Biology*, *17*(6), 379–394.

Shintomi, K., & Hirano, T. (2009). Releasing cohesin from chromosome arms in early mitosis: Opposing actions of Wapl-Pds5 and Sgo1. *Genes and Development*, *23*(18), 2224–2236.

Silver, L. M. (1995). Karyotypes, Chromosomes and Translocations. *Mouse Genetics: Concepts and Applications*, 83–92. ISBN-978-0-19-507554-0

Smith, K. N., Penkner, A., Ohta, K., Klein, F., & Nicolas, A. (2001). B-type cyclins CLB5 and CLB6 control the initiation of recombination and synaptonemal complex formation in yeast meiosis. *Current Biology*, *11*(2), 88–97. ^

Springer, M. S., Goy, M. F., & Adler, J. (1979). Protein methylation in behavioural control mechanisms and in signal transduction. *Nature*, *280*, 279–284.

Stansel, R. M., Lange, T. De, & Grif, J. D. (2001). T-loop assembly in vitro involves binding of TRF2 near the 3' telomeric overhang. *The EMBO Journal*, *20*(19).

Strunnikov, A. V., & Jessberger, R. (1999). Structural maintenance of chromosomes (SMC) proteins: Conserved molecular properties for multiple biological functions. *European Journal of Biochemistry*, *263*(1), 6–13.

Sun, X., & Cohen, P. E. (2013). Studying Recombination in Mouse Oocytes. In H. A. Homer (Ed.), *Mammalian Oocyte Regulation* (pp. 1–18). Springer Science+Business Media. ISBN- 978-1-62703-190-5

Syrjänen, J. L., Pellegrini, L., & Davies, O. R. (2014). A molecular model for the role of SYCP3 in meiotic chromosome organization. *eLIFE*, *3*(e02963), 1–18.

Tachibana-Konwalski, K., Godwin, J., Van Der Weyden, L., Champion, L., Kudo, N. R., Adams, D. J., & Nasmyth, K. (2010). Rec8-containing cohesin maintains bivalents without turnover during the growing phase of mouse oocytes. *Genes and Development*, *24*(22), 2505–2516.

Tessarz, P., Santos-Rosa, H., Robson, S. C., Sylvestersen, K. B., Nelson, C. J., Nielsen, M. L., & Kouzarides, T. (2014). Glutamine methylation in histone H2A is an RNA-polymerase-I-dedicated modification. *Nature*, *505*(7484), 564–8.

Tóth, A., Ciosk, R., Uhlmann, F., Galova, M., Schleiffer, A., & Nasmyth, K. (1999). Yeast cohesin complex requires a conserved protein, Eco1p(Ctf7), to establish cohesion between sister chromatids during DNA replication. *Genes and Development*, *13*(3), 320–333.

Toth, A., & Jessberger, R. (2016). Oogenesis: Ageing Oocyte Chromosomes Rely on Amazing Protein Stability. *Current Biology*, *26*(8), R329–R331.

Uhlmann, F., & Nasmyth, K. (1998). Cohesion between sister chromatids must be established during DNA replication. *Current Biology*, *8*, 1095–1101.

Ulrich, H. D. (2002). Degradation or maintenance: Actions of the ubiquitin system on eukaryotic chromatin. *Eukaryotic Cell*, *1*(1), 1–10.

Unal, E., Heidinger-Pauli, J.M., Kim W, Guacci V, Onn I, Gygi SP, K. D. (2008). A molecular determinant for the establishment of sister chromatid cohesion. *Science*, *321*(5888), 566-9.

Van Steensel, B., Smogorzewska, A., & De Lange, T. (1998). TRF2 protects human telomeres from end-to-end fusions. *Cell*, *92*(3), 401–413.

Vernì, F., Gandhi, R., Goldberg, M. L., & Gatti, M. (2000). Genetic and molecular analysis of wings apart-like (wapl), a gene controlling heterochromatin organization in Drosophila melanogaster. *Genetics*, *154*(4), 1693–1710.

Voges D., Zwickl P., B. W. (1999). The 26S proteasome: a molecular machine designed for controlled proteolysis. *Annu Rev Biochem.*, *68*, 1015–1068.

Von Stetina, J. R., & Orr-Weaver, T. L. (2011). Developmental control of oocyte maturation and egg activation in metazoan models. *Cold Spring Harbor Perspectives in Biology*, *3*(10), 1–19.

Walker, J. R., & Zhu, X. D. (2012). Post-translational modifications of TRF1 and TRF2 and their roles in telomere maintenance. *Mechanisms of Ageing and Development*, *133*(6), 421–434.

Wang, F., Yoder, J., Antoshechkin, I., & Han, M. (2003). Caenorhabditis elegans EVL-14/PDS-5 and SCC-3 are essential for sister chromatid cohesion in meiosis and mitosis. *Molecular and Cellular Biology*, *23*(21), 7698–707.

Watanabe, Y. (2012). Geometry and force behind kinetochore orientation: lessons from meiosis. *Nature Reviews Molecular Cell Biology*, *13*(6), 370–382.

Watanabe, Y., & Nurse, P. (1999). Cohesin Rec8 is required for reductional chromosome segregation at meiosis, *400*(July), 1997–2000.

Wilkinson, K. D. (1997). Regulation of ubiquitin-dependent processes by deubiquitinating enzymes. *The FASEB Journal : Official Publication of the Federation of American Societies for Experimental Biology*, *11*(14), 1245–1256.

Yang F1, W. P. (2009). The Mammalian synaptonemal complex: a scaffold and beyond. *Genome Dyn. 5*, 69-80.

Yang, F., De La Fuente, R., Leu, N. A., Baumann, C., McLaughlin, K. J., & Wang, P. J. (2006). Mouse SYCP2 is required for synaptonemal complex assembly and chromosomal synapsis during male meiosis. *Journal of Cell Biology*, *173*(4), 497–507.

Yoshimi, K., Kunihiro, Y., Kaneko, T., Nagahora, H., Voigt, B., & Mashimo, T. (2016). ssODN-mediated knock-in with CRISPR-Cas for large genomic regions in zygotes. *Nature Communications*, *7*, 10431.

Yuan, L., Liu, J.-G., Hoja, M.-R., Wilbertz, J., Nordqvist, K., & Hoog, C. (2002). Female Germ Cell Aneuploidy and Embryo Death in Mice Lacking the Meiosis-Specific Protein SCP3. *Science*, *296*(May), 1115–1119.

Zhang, B., Jain, S., Song, H., Fu, M., Heuckeroth, R. O., Erlich, J. M., Jay, P. J., Milbrandt, J. (2007). Mice lacking sister chromatid cohesion protein PDS5B exhibit developmental abnormalities reminiscent of Cornelia de Lange syndrome. *Development (Cambridge, England)*, *134*(17), 3191–3201.

Zhang, J., Shi, X., Li, Y., Kim, B. J., Jia, J., Huang, Z., Yang, T., Fu, X., Jung, S. Y., Wang, Y., Zhang, P., Kim, S. T., Pan, X., Qin, J. (2008). Acetylation of Smc3 by Eco1 Is Required for S Phase Sister Chromatid Cohesion in Both Human and Yeast. *Molecular Cell*, *31*(1), 143–151.

Zhang, X., Wen, H., & Shi, X. (2012). Lysine methylation : beyond histones Modifying Enzymes for Lysine Methylation. *Acta Biochim Biophys Sin*, *44*, 14–27.

Zhao, S., Xu, W., Jiang, W., Yu, W., Lin, Y., Zhang, T., Yao, J., Zhou, L., Zeng, Y., Li, H., Li, Y., Shi, J., An, W., Hancock, S. M., He, F., Qin, L., Chin, J., Yang, P., Chen, X., Lei, Q., Xiong, Y., Guan, K. (2013). Regulation of Cellular Metabolism by Protein Lysine Acetylation, *340*(April), 216–219.

Table of figures

Appendix

Abstract

Holding together replicated sister chromatids is an essential requirement for proper chromosome segregation during mitosis and meiosis. This so-called sister chromatid cohesion is established through cohesin, a ring-like multiprotein complex that embraces double-stranded DNA. Due to the prolonged meiotic cell cycle of mammalian females, sister chromatid cohesion needs to be maintained for weeks or months in mice or in humans for years or decades. This presupposes a tight regulation of factors responsible for chromatid cohesion in order to preserve the genomic integrity of a healthy oocyte. One essential component of the mice meiotic cohesin complex is Smc1β. Smc1β is thought to be involved in meiotic recombination and required for maintenance of sister chromatid cohesion. How meiotic cohesin is regulated by post-translational modifications in mammalian meiosis is not known. Using mouse genetics, we show that specific residues that are post-translationally modified are necessary for Smc1β's function in meiotic recombination and centromeric cohesion. We find that Smc1β affects crossover distribution and efficiency of crossover maturation in fetal oocytes. Smc1β is required for close association of sister-kinetochores in meiosis I diakinesis oocytes, suggesting that it is involved in centromeric cohesion. Thus, our study provides insights into the regulation of Smc1β-containing cohesin complex. We propose that post-translational modifications regulate the function of the meiotic cohesin complex during meiotic recombination and sister chromatid cohesion.

Zusammenfassung

Um eine korrekte Chromosomenverteilung während Mitose und Meiose zu ermöglichen, müssen neu replizierte Schwesterchromatiden eng zusammengehalten werden. Dieser Zusammenhalt, genannt Kohäsion, wird gewährleistet durch das binden von Multiprotein Cohesin Komplexen an doppelsträngige DNA, um sie so ringförmig zu umschließen und zu verknüpfen. Aufgrund des verzögerten meiotischen Zellzyklus in weiblichen Organismen, muss die Schwesterchromatidenkohäsion in Mäusen für Wochen oder Monate und im Menschen sogar über Jahre oder Jahrzehnte sichergestellt werden. Um die Integrität einer gesunden Eizelle zu schützen, müssen Cohesin Komplexe so lange gebunden bleiben, bis der meiotische Zellzyklus fortsetzt wird, was wiederum eine strenge Regulation von Cohesin vorraussetzt. Ein essentielles Protein, genannt Smc1β, wurde als Bestandteil von Cohesin in Mäusen identifiziert. Aufgrund bisheriger Studien wird vermutet, dass Smc1β eine Funktion während der meiotischen Rekombination erfüllt und für den Erhalt der Kohäsion der Schwesterchromatiden erforderlich ist. Wie der meiotische Cohesin Komplex in Säugetieren durch post-translationale Proteinmodifikationen reguliert wird, ist nicht bekannt. Wir zeigen, dass bestimmte post-translational modifizierte Aminosäuren in Smc1β notwendig sind, um seine Funktion während der meiotischen Rekombination zu erfüllen und Schwestercentromere zusammenzuhalten. Wir beobachten eine Rolle von Smc1β während der Verteilung und effizienten Reifung von Cross-overs in fötalen Eizellen. Smc1b ist notwendig für die korrekte Assoziation von Schwesterkinetochoren von Chromosomen während der Diakinese. Dies lässt auf eine Rolle von Smc1b in centromerer Kohäsion schließen. Unsere Studie gewährt Einblicke in die Regulierung von Cohesin Komplexen, welche Smc1β enthalten. Wir schlussfolgern, dass post-translationale Modifikationen die Funktion der meiotischen Cohesin Komplexe während meiotischer Rekombination und Schwesterchromatidenkohäsion regulieren.